Water Research 157 (2019) 514–528

Contents lists available at ScienceDirect

Water Research

journal homepage: www.elsevier.com/locate/watres

Reactions of aliphatic amines with ozone: Kinetics and mechanisms

Sungeun Lim [a, b], Christa S. McArdell [a], Urs von Gunten [a, b, *]

[a] Eawag, Swiss Federal Institute of Aquatic Science and Technology, Ueberlandstrasse 133, 8600, Duebendorf, Switzerland
[b] School of Architecture, Civil and Environmental Engineering (ENAC), École Polytechnique Fédérale de Lausanne (EPFL), 1015, Lausanne, Switzerland

ARTICLE INFO

Article history:
Received 29 November 2018
Received in revised form
13 March 2019
Accepted 27 March 2019
Available online 29 March 2019

Keywords:
Aliphatic amines
Ozone
Reaction kinetics
Reaction mechanisms
Transformation products
Nitroalkanes

ABSTRACT

Aliphatic amines are common constituents in micropollutants and dissolved organic matter and present in elevated concentrations in wastewater-impacted source waters. Due to high reactivity, reactions of aliphatic amines with ozone are likely to occur during ozonation in water and wastewater treatment. We investigated the kinetics and mechanisms of the reactions of ozone with ethylamine, diethylamine, and triethylamine as model nitrogenous compounds. Species-specific second-order rate constants for the neutral parent amines ranged from 9.3×10^4 to $2.2 \times 10^6\ M^{-1}s^{-1}$ and the apparent second-order rate constants at pH 7 for potential or identified transformation products were $6.8 \times 10^5\ M^{-1}s^{-1}$ for *N,N*-diethylhydroxylamine, $\sim 10^5\ M^{-1}s^{-1}$ for *N*-ethylhydroxylamine, $1.9 \times 10^3\ M^{-1}s^{-1}$ for *N*-ethylethanimine oxide, and $3.4\ M^{-1}s^{-1}$ for nitroethane. Product analyses revealed that all amines were transformed to products containing a nitrogen-oxygen bond (e.g., triethylamine *N*-oxide and nitroethane) with high yields, i.e., 64–100% with regard to the abated target amines. These findings could be confirmed by measurements of singlet oxygen and hydroxyl radical which are formed during the amine-ozone reactions. Based on the high yields of nitroethane from ethylamine and diethylamine, a significant formation of nitroalkanes can be expected during ozonation of waters containing high levels of dissolved organic nitrogen, as expected in wastewaters or wastewater-impaired source waters. This may pose adverse effects on the aquatic environment and human health.

1. Introduction

Ozone has been used as a disinfectant and/or oxidant in water and wastewater treatment since the early 20th century (von Sonntag and von Gunten, 2012). It has a significant potential for the abatement of micropollutants in drinking waters and also recently in wastewater effluents (Eggen et al., 2014; Tentscher et al., 2018; Ternes et al., 2003; von Gunten, 2018). In general, ozonation reduces the overall toxicity exerted by micropollutants by eliminating or altering the moieties responsible for biological activities (Dodd et al., 2009; Lee et al., 2008; Mestankova et al., 2011). However, an increased toxicity has also been observed in ozone-treated waters (Magdeburg et al., 2014; Stalter et al., 2010; von Gunten, 2018). This resulted mainly from the reaction of ozone with dissolved organic matter (DOM), thereby forming byproducts such as quinones (Tentscher et al., 2018), low molecular weight organic carbon compounds (Hammes et al., 2006; Ramseier et al., 2011), and compounds containing nitrogen-oxygen bonds (McCurry et al., 2016). Micropollutants can also be transformed to toxic transformation products upon ozonation, but their contribution to the overall toxicity is expected to be smaller, as DOM is present in much higher concentrations than micropollutants in real water matrices and consumes by far the largest fraction of the oxidants (von Gunten, 2018). Toxic oxygen-containing products, whether they are byproducts from DOM or transformation products from micropollutants, are typically expected to be removed by biological post-treatment (Hammes et al., 2006). However, some products (e.g., *N*-oxides) are persistent even during a biological post-treatment step (Bourgin et al., 2018; Hübner et al., 2015). To better understand the formation of persistent transformation products or byproducts, many studies have been conducted to reveal their formation pathways (Krasner et al., 2013; Shah and Mitch, 2012) and to identify transformation products (Hübner et al., 2015; von Sonntag and von Gunten, 2012). Recently, computational tools have been developed based on the current kinetic/mechanistic knowledge to predict ozone exposure, reaction kinetics, and transformation products upon ozonation (Lee et al., 2017; Lee and von Gunten, 2016). A successful implementation of

* Corresponding author. Eawag, Swiss Federal Institute of Aquatic Science and Technology, Ueberlandstrasse 133, 8600, Duebendorf, Switzerland.
E-mail address: vongunten@eawag.ch (U. von Gunten).

https://doi.org/10.1016/j.watres.2019.03.089
0043-1354/

such prediction tools will depend on the quality of the underlying reaction mechanisms which ideally cover a comprehensive compilation of ozone-reactive moieties. A considerable wealth of information is available for the reactions of ozone with ozone-reactive moieties such as olefins, aromatic compounds, and sulfur-containing compounds, and the relevant information is also well documented (von Gunten, 2018; von Sonntag and von Gunten, 2012). However, there is less information on the ozone-reactivity of nitrogenous compounds and a need for a more fundamental understanding of the corresponding reaction mechanisms.

Aliphatic amines, one of the simplest forms of nitrogen-containing compounds, are common constituents of dissolved organic nitrogen (DON) (Westerhoff and Mash, 2002). Understanding the reactions of aliphatic amines with ozone has been important, because, due to water scarcity, water suppliers increasingly use impaired water resources with higher levels of DON. Such sources are surface waters impacted by wastewater discharge, agricultural activities, or algal blooms (Graeber et al., 2015; Pehlivanoglu-Mantas and Sedlak, 2006; Westerhoff and Mash, 2002) and wastewater effluents treated for the purpose of direct potable reuse (Leverenz et al., 2011). Aliphatic amines are also commonly found as functional groups in many organic micropollutants. From a list of 550 environmentally relevant substances (Bourgin et al., 2018), more than 80% of micropollutants contain a nitrogen and about a quarter of the nitrogen-containing micropollutants are categorized as aliphatic amines. Aliphatic amines in their neutral forms react fast with ozone due to the lone electron pair on the nitrogen atom susceptible to an electrophilic attack by ozone with second-order rate constants $k_{O3} = 10^3–10^7\ M^{-1}s^{-1}$ (von Sonntag and von Gunten, 2012). Certain primary and secondary amines have the potential to be transformed to harmful products such as *N*-nitrosodimethylamine with low yields of less than 0.02% upon ozonation (Andrzejewski et al., 2008; Yang et al., 2009) and chloropicrin with ~50% yield upon ozonation followed by post-chlorination (McCurry et al., 2016). These nitrogenous disinfection byproducts (e.g., *N*-nitrosamines, halonitroalkanes) are significantly more toxic than regulated disinfection byproducts (e.g., trihalomethanes, haloacetic acids), wherefore the formation of the nitrogenous disinfection byproducts has gained increasing attention recently (Bond et al., 2012, 2011; Shah and Mitch, 2012). Despite the great relevance of aliphatic amines to the ozone chemistry in water and wastewater treatment (common moieties, high reactivity towards ozone, potential of harmful products), their reactions with ozone have not been entirely elucidated. In-depth investigations on ozone-amine reactions were reported by Bailey in the 1960s - 1970s but most experiments were carried out in organic solvents (Bailey and Keller, 1968; Bailey et al., 1978). Current knowledge on amine-ozone reactions in aqueous solutions is mostly limited to tertiary amines. *N*-oxides have often been detected as major products during ozonation of micropollutants containing a tertiary amine moiety (Borowska et al., 2016; Knoop et al., 2018; Lange et al., 2006; Lester et al., 2013; Muñoz and von Sonntag, 2000a; Zimmermann et al., 2012). Accordingly, the principal mechanism of the reaction of tertiary amines with ozone has been proposed as an oxygen transfer reaction where ozone initially attacks a tertiary amine nitrogen to form a $-N^+-O-O-O^-$ adduct which further dissociates into a *N*-oxide and singlet oxygen (von Sonntag and von Gunten, 2012). Alternatively, tertiary amines can react with ozone via an electron transfer pathway to yield an aminyl radical cation and an ozonide radical anion. The ensuing radicals further dissociate into a *N*-dealkylated amine and a hydroxyl radical, respectively (von Sonntag and von Gunten, 2012). For the reaction of secondary amines with ozone, hydroxylamines (an analogous product to *N*-oxides for tertiary amines) and primary amines were identified as products, but there is only limited molar yield information (Benner and Ternes, 2009a, 2009b; Tekle-Röttering et al., 2016; von Gunten, 2003). For the reaction of primary amines with ozone, nitrate and ammonia were identified as final products (Berger et al., 1999; de Vera et al., 2017; Le Lacheur and Glaze, 1996), but the studies were conducted under ozone excess conditions and the initial ozonation products of primary amines are still unknown.

The aim of this study was to investigate the chemistry of the ozone-amine reactions for simple aliphatic amines such as ethylamine, diethylamine, and triethylamine. The second-order rate constants for the reactions of the model compounds with ozone, transformation products and reactive oxygen species (singlet oxygen and hydroxyl radical) were determined by various experimental approaches and analytical methods. In addition, kinetic experiments/simulations and quantum chemical computations were performed. Based on these results, reaction mechanisms for primary, secondary and tertiary amines were proposed, allowing a comprehensive assessment of the fate of these moieties during ozonation.

2. Materials and methods

Chemical reagents. Chemicals and suppliers are listed in Table S1 in the supporting information. *N*-ethylethanimine oxide was synthesized at Eawag (Text S1) and UV–vis spectra of this compound were recorded as received ($\lambda_{max} = 224$ nm). Working stocks of *N*-ethylethanimine oxide were freshly made every day and the concentrations were determined based on the absorbance at 224 nm (Fig. S1).

Ozonation experiments. Ozone stock solutions were prepared by sparging ozone-containing oxygen through ultrapure water kept on ice (Bader and Hoigné, 1981). The concentration of ozone in the stock solution (1.3–1.5 mM) was determined spectrophotometrically based on the molar absorption coefficient of ozone, $\varepsilon = 3200\ M^{-1}cm^{-1}$ at 260 nm (von Sonntag and von Gunten, 2012). An aliquot of the ozone stock solution was added to the solution containing the target amine compound to initiate the ozone reaction with doses ranging from 0 to 300 μM. The solutions of the model compounds (ethylamine, diethylamine, *N*,*N*-diethylhydroxylamine, *N*-ethylethanimine oxide, or triethylamine; initial concentrations ~100 μM) were prepared in 10 mM phosphate buffer at pH 7. 50 mM of *t*-butanol was present in the solutions as a hydroxyl radical scavenger to suppress unwanted side reactions associated with hydroxyl radical. The ozonated samples were typically allowed to react for 24 h at room temperature to ensure a complete consumption of ozone and stored at 4 °C for less than a week prior to further analyses.

Reaction kinetics. Second-order rate constants for the reactions of the model compounds and their transformation products with ozone in the pH range far below the pK_a of the amines were determined by a direct measurement of the ozone decrease with the indigo reagent (Text S2) (Bader and Hoigné, 1981). Under these conditions, the amines were predominantly present in the protonated form, which lowered the reaction kinetics sufficiently to allow measurements by a direct method. The species-specific second-order rate constants for the neutral amines were then obtained by extrapolating the determined apparent second-order rate constants to a higher pH (Hoigné and Bader, 1983). Additionally, a competition kinetic method with cinnamic acid as a competitor (Leitzke et al., 2001) was used for determining apparent second-order rate constants of *N*,*N*-diethylhydroxylamine at pH 5–8, which are too high to be determined by the direct method.

Analytical methods. Diethylamine, *N*-ethylethanimine oxide, triethylamine, triethylamine *N*-oxide were analyzed by liquid chromatography coupled with high resolution tandem mass

spectrometry (LC-HRMS/MS) and nitroethane was analyzed by GC-MS. Ethylamine was derivatized with 9-fluorenylmethylchloroformate and the derivatized product was analyzed by HPLC-UV (Jámbor and Molnár-Perl, 2009). Nitrite and nitrate were determined by ion chromatography with conductivity detection. All chromatographic conditions and detection methods including the limits of quantification and the measuring ranges are provided in detail in Text S3 and Table S2. Singlet oxygen was quantified by a near-infrared photomultiplier tube which directly measured a characteristic phosphorescence of singlet oxygen emitted at 1270 nm. The setup and the reference reaction to calibrate the instrument were adapted from a previous study (Muñoz et al., 2001) and described in Text S4. Hydroxyl radicals were indirectly quantified by measuring the concentration of formaldehyde, a known product of the reaction of hydroxyl radicals with *t*-butanol (Flyunt et al., 2003; Nöthe et al., 2009). Formaldehyde was quantified by derivatization with 2,4-dinitrophenylhydrazine followed by HPLC-UV analysis (Text S5) (Lipari and Swarin, 1982). Hydrogen peroxide was indirectly quantified by measuring singlet oxygen formation after adding hypochlorous acid to the samples containing hydrogen peroxide (Text S6) (Tentscher et al., 2018).

Quantum chemical computations. All computations were conducted by the Gaussian 09 program (Revision D.01) (Frisch et al., 2016). Gas phase electronic energies of all molecules were computed by the CCSD(T) functional (Raghavachari et al., 1989) with the jul-cc-pVTZ basis set (Papajak et al., 2011). Aqueous Gibbs free energies were calculated by adding gas phase thermal corrections (computed by B3LYP/CBSB7) (Becke, 1993; Montgomery et al., 1999) and solvation effects (by M062X/6-31G*) (Hariharan and Pople, 1973; Marenich et al., 2009; Zhao and Truhlar, 2008) to the gas phase electronic energies. More details are provided in Text S8.

3. Results and discussion

The mechanisms for the reactions of ozone with aliphatic amines were elucidated as follows: (1) Determination of apparent and species-specific second-order rate constants for the reactions of the selected amines with ozone, (2) identification/quantification of transformation products and (3) reactive oxygen species ($^1O_2$ and •OH) formed during the amine-ozone reactions, (4) quantum chemical computations, and (5) kinetic simulations. In the following these aspects are discussed and compiled to overall proposed reaction mechanisms.

3.1. Ozone kinetics

Apparent second-order rate constants for the reactions of ethylamine, diethylamine, and triethylamine with ozone were determined in the pH range 3–7. Based on this, the species-specific second-order rate constants were calculated and are summarized in Table 1. The species-specific second-order rate constants for the reactions of ozone with the neutral amines are in the range of 9.3×10^4 to $2.2 \times 10^6\ M^{-1}s^{-1}$. They are comparable to literature values within a factor of 2.6, an acceptable deviation commonly found among kinetic studies. At pH 7, the apparent second-order rate constants ($k_{obs,pH7}$) for the ozone reactions with all amines were 3–4 orders of magnitude lower because the protonated amines (pK_a values 10.5–11.0) which are dominant at pH 7, are practically unreactive with ozone. The second-order rate constants for the reactions of potential or identified transformation products were also determined. *N,N*-diethylhydroxylamine, a potential product from the diethylamine-ozone reaction, was very reactive at pH 7 due to its lower pK_a (5.4, see below) compared to other amines, which leads to an almost 100% fraction of the neutral amine species at this pH. The pK_a of *N,N*-diethylhydroxylamine was estimated by fitting the apparent second-order rate constants determined in the pH range 1.6–8.0 to an expression for the species-specific second-order rate constant. This includes the degree of dissociation of the amine at a given pH and the corresponding species-specific rate constants, i.e., $k = k_{NH+}(1\text{-}\alpha) + k_N\alpha$ and $\alpha = 1/(1 + 10^{pKa\text{-}pH})$, where k_{NH+} and k_N are the species-specific second-order rate constants for the protonated and the neutral amines, respectively, and α is the fraction of the neutral amine. As a result of the fitting (shown in Fig. S2), the estimated pK_a value is 5.4, similar to the predicted value of 5.7 determined by a commercial pK_a prediction software (ACD/Labs, V 11.02) (https://www.acdlabs.com). The species-specific second-order rate constant of *N,N*-diethylhydroxylamine was estimated as $7.0 \times 10^5\ M^{-1}s^{-1}$. *N*-ethylhydroxylamine, a potential product from the ethylamine-ozone reaction, was also very reactive at pH 7. The estimated apparent second-order rate constant at pH 7 ($k_{obs,pH7}$) was ~$10^5\ M^{-1}s^{-1}$, based on the measured apparent second-order rate constants at pH 2 and 4 and a predicted pK_a value of 6.2 (ACD/Labs, V 11.02). The $k_{obs,pH7}$ is only a rough estimate because only two pH conditions

Table 1
Species-specific and apparent second-order rate constants for the reactions of the selected amines with ozone and pK_a values of the amines.

Compound	pK_a	Method[c]	pH[d]	k, $M^{-1}s^{-1}$	$k_{obs,pH7}$, $M^{-1}s^{-1}$	Reference
Ethylamine	10.6	Indigo	5.0–7.0	$(9.3 \pm 0.1) \times 10^4$	21	This study
				2.4×10^5		Muñoz and von Sonntag (2000a)
Diethylamine	10.5	Indigo	3.0–7.0	$(3.9 \pm 0.1) \times 10^5$	1.3×10^2	This study
				6.2×10^5		Pryor et al. (1984)
				9.1×10^5		Muñoz and von Sonntag (2000a)
Triethylamine	11.0	Indigo	4.0–6.5	$(2.2 \pm 0.1) \times 10^6$	2.2×10^2	This study
				2.1×10^6		Pryor et al. (1984)
				4.1×10^6		Muñoz and von Sonntag (2000a)
N,N-Diethylhydroxylamine	5.4[a]	Indigo; CK	1.6–8.0	$(7.0 \pm 0.02) \times 10^5$	6.8×10^5	This study
N-ethylhydroxylamine	6.2[b]	Indigo	2 and 4	ND	~10^5	This study
N-ethylethanimine oxide	NA	Indigo	7.0 only	ND	$(1.9 \pm 0.04) \times 10^3$	This study
Nitroethane	NA	Indigo	7.0 only	ND	3.4 ± 0.1	This study

[a] pK_a of *N,N*-diethylhydroxylamine was estimated from the apparent second-order rate constants measured at varying pH conditions (see the fitting equation and the results in Text S2 and Fig. S2).
[b] pK_a of *N*-ethylhydroxylamine was predicted by a commercial software (ACD/Labs, V11.02) (https://www.acdlabs.com).
[c] Reaction kinetics were determined by direct monitoring of the ozone decrease with the indigo method (indigo) or by competition kinetics with cinnamic acid (CK) as described in detail in Text S2.
[d] Experimental pH range.

were applied. The reaction kinetics of *N*-ethylethanimine oxide, an identified product from the reactions of diethylamine and triethylamine with ozone, was determined with a fresh *N*-ethylethanimine oxide solution prepared *in situ* to minimize the impact of dimers on the reaction kinetics (Text S2). *N*-ethylethanimine oxide was moderately reactive to ozone at pH 7 with an apparent second-order rate constant at pH 7, $k_{obs,pH7} = 1.9 \times 10^3\ M^{-1}s^{-1}$. Nitroethane, identified as a final product from all amine-ozone reactions, reacted slowly with ozone with an apparent second-order rate constant at pH 7, $k_{obs,pH7} = 3.4\ M^{-1}s^{-1}$.

3.2. Product analyses and reaction mechanisms

3.2.1. Triethylamine-ozone reaction

Transformation products. The abatement of triethylamine and the evolution of transformation products as a function of the ozone doses were measured in presence of *t*-butanol as a hydroxyl radical scavenger (Fig. 1a). All compounds presented in Fig. 1 were quantified by various analytical methods with reference standards (Text S3). Triethylamine (94 μM initial concentration) gradually decreased for ozone doses of ≤100 μM and was completely abated for an ozone dose of ~110 μM, yielding a molar ozone:triethylamine reaction stoichiometry of about 1. The major product was triethylamine *N*-oxide, in agreement with previous findings from reactions of tertiary amines with ozone in laboratory- and full-scale studies (Borowska et al., 2016; Bourgin et al., 2018; Knoop et al., 2018; Lange et al., 2006; Muñoz and von Sonntag, 2000a; von Sonntag and von Gunten, 2012; Zimmermann et al., 2012). A minor product is nitroethane, which was formed in small concentrations but gradually built up with increasing ozone doses. Triethylamine *N*-oxide and nitroethane were final products with yields of 87% and 9%, respectively, based on the abated triethylamine at the highest applied ozone dose (300 μM). Diethylamine and *N*-ethylethanimine oxide were formed as transient products to a lesser extent (insert of Fig. 1a) and were subsequently degraded at high ozone doses, likely concomitant with the formation of nitroethane (see section 3.2.2). The sum of the concentrations of all nitrogen species is presented as a mass balance in Fig. 1a. The mass balance was maintained at 89–110% for all ozone doses. As this is a very reasonable mass balance for a product study, it can be concluded that no major transformation products are missing for the ozone-induced transformation of triethylamine.

Reactive oxygen species. The reaction of triethylamine with ozone exerted a high yield of $^1O_2$ (70% of the consumed ozone, Table 2). In contrast, the •OH yield was only 6.4%. These yields are roughly within the same range compared to previously reported

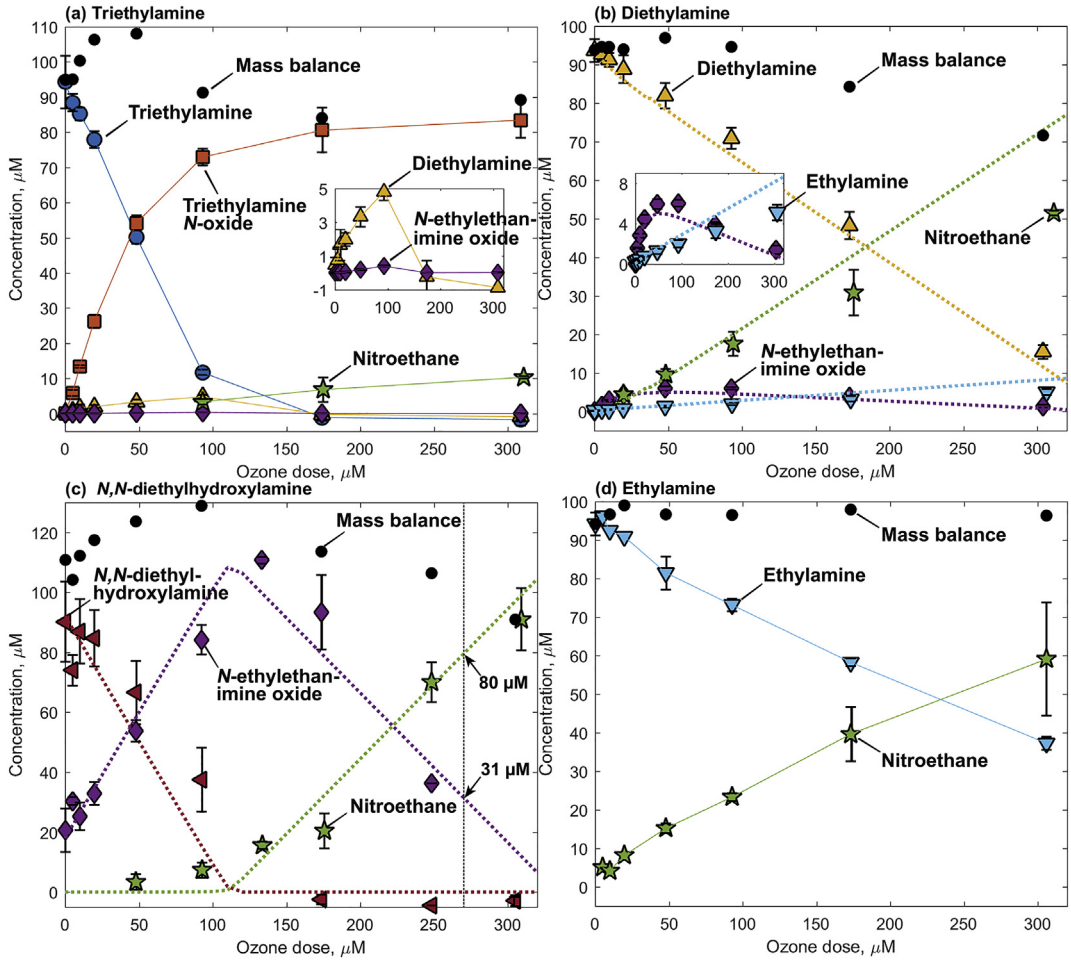

Fig. 1. Evolution of the amine model compounds and transformation products as a function of the ozone doses for the reactions of ozone with (a) triethylamine, (b) diethylamine, (c) *N,N*-diethylhydroxylamine, and (d) ethylamine. Inserts in (a) and (b) have the same axis labels as the main plots. The symbols indicate measured concentrations (duplicate or triplicate) and the dotted lines in (b) and (c) indicate simulated concentrations based on the kinetic models described in Table S7 and Table S5, respectively. The vertical line in (c) is at an ozone dose of 270 μM. The errors were calculated as standard deviations. Experimental conditions: $[amine]_0$ = 100 μM, [ozone] = 0–300 μM, [*t*-butanol] = 50 mM, 10 mM phosphate buffer (pH 7), and reaction time = 24 h (triethylamine, diethylamine, and ethylamine) or 3–5 h (*N,N*-diethylhydroxylamine).

Table 2
Yields of reactive oxygen species ($^1O_2$ and •OH) per consumed ozone at an amine:ozone ratio of 1:1 (yields for other ratios are given in Table S3 and Fig. S12). Ozone concentrations were 0.1 or 0.4–0.5 mM for $^1O_2$ measurements and 0.09 mM for •OH measurements. All measurements were performed at pH 7, except for $^1O_2$ formation from ethylamine (pH 9). *t*-Butanol was added for all $^1O_2$ measurements carried out in this study. Yields were averaged for 5–9 replicates for $^1O_2$ and duplicates for •OH and standard deviations were within 10% of the average values.

Compound	Type	$^1O_2/O_3$	Reference	•OH/O_3	Reference
Triethylamine	Tertiary amine	0.70	This study	0.064	This study
		0.80[a]	Muñoz et al. (2001)	0.15	Flyunt et al. (2003)
Diethylamine	Secondary amine	0.46	This study	0.26	This study
		0.20[b]	Muñoz et al. (2001)		
Piperidine		–		0.28	Tekle-Röttering et al. (2016)
Ethylamine	Primary amine	0.27	This study	0.33	This study
		0.17[b]	Muñoz et al. (2001)		
Glycine		–		0.25	de Vera et al. (2017)
N,N-diethylhydroxylamine	Hydroxylamine	0.38	This study	0.43	This study
N-ethylethanimine oxide	Nitrone	0.43[c]	This study	0.43[c]	This study

[a] Without *t*-butanol, pH 8, and molar amine:ozone = 100.
[b] Without *t*-butanol, pH 10.5, and molar amine:ozone = 10.
[c] Possibly influenced by the presence of a dimer.

values of 80% for $^1O_2$ and 15% for •OH (Flyunt et al., 2003; Muñoz et al., 2001). The previously reported $^1O_2$ yields were determined without *t*-butanol. Nevertheless, the yields determined under amine-excess conditions (amine:ozone ≥ 10) (Muñoz et al., 2001) can be compared to our results because the effect of •OH on amine and ozone concentrations is minimal under these conditions despite the absence of an •OH scavenger. We also measured $^1O_2$ yields for conditions with the amine in excess without *t*-butanol and obtained comparable results (70%, Table S3). The yields of $^1O_2$ and •OH correspond well to the product formation trend where triethylamine *N*-oxide (yielding $^1O_2$) was observed in much higher concentrations than the dealkylated amine, diethylamine (yielding •OH) and its identified transformation products, nitroethane (see section 3.2.2). Both results from the formation of transformation products and the detection of reactive oxygen species indicate that the reaction of triethylamine with ozone predominantly occurs via oxygen transfer forming triethylamine *N*-oxide and $^1O_2$ rather than via electron transfer forming diethylamine and •OH.

Reaction pathways. The experimental findings on the triethylamine-ozone reactions are described well by two pathways: The formation of triethylamine *N*-oxide and $^1O_2$ via an oxygen transfer and the formation of diethylamine and •OH via an electron transfer mechanism (Fig. 2). The extent of oxygen transfer and electron transfer was further elucidated by calculating the yields of transformation products and reactive oxygen species. The concentrations of the products were divided by the concentrations of abated triethylamine determined at an ozone dose of 93 μM (Δ[Triethylamine] = 83 μM) and expressed in percentage in Fig. 2. For the reactive oxygen species, the yields determined with regard to consumed ozone in Table 2 were converted to the yields per abated triethylamine to be comparable with the transformation product yields (e.g., the converted $^1O_2$ yield = $(^1O_2/O_3) \times [O_3]/\Delta$[Triethylamine] = 0.70 × 93μM/83 μM = 78%). In summary, of the abated 83 μM of triethylamine at 93 μM of ozone, 88 ± 3% was transformed into triethylamine *N*-oxide and 5 ± 1% into diethylamine. The yields of reactive oxygen species matched quite well the yields of the transformation product counterparts, namely 78 ± 3% of $^1O_2$ and 7 ± 0.3% of •OH.

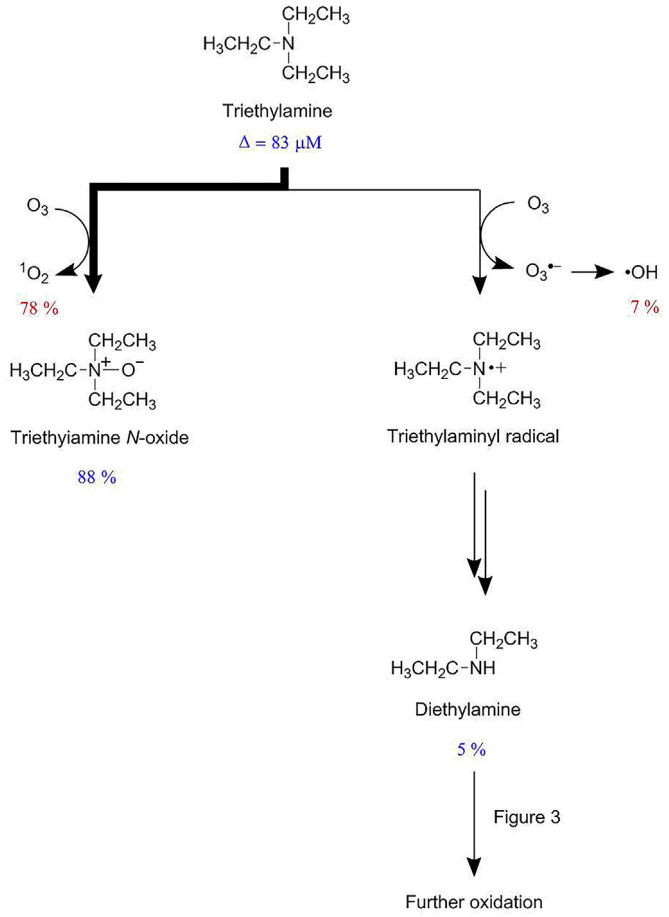

Fig. 2. Proposed mechanism for the reaction of triethylamine with ozone. Product yields (in %) were calculated by dividing the measured concentrations of the transformation products and the reactive oxygen species by the abated triethylamine (83 μM) at an ozone dose of 93 μM. The bold arrow indicates the major pathway of the branched reaction.

3.2.2. Diethylamine-ozone reaction

Transformation products. Fig. 1b shows the abatement of diethylamine and the corresponding product formation upon ozonation. In contrast to triethylamine, diethylamine required a much higher specific ozone dose with a molar stoichiometry ozone:diethylamine of about 4 for a complete abatement. Nitroethane, a highly oxidized form of nitrogen with an oxidation state of +3 (in comparison to −3 of diethylamine), was the major product with a 64% yield based on the diethylamine abatement at 300 μM ozone. *N*-ethylethanimine oxide and ethylamine were additionally detected as minor products with yields of 2% and 7%, respectively, at 300 μM ozone (insert in Fig. 1b). *N*-ethylethanimine oxide is a *N*-oxide of an imine derivative of diethylamine and belongs to the

class of nitrones. *N*-ethylethanimine oxide was formed in small quantities for ozone doses ≤100 μM and was abated again for higher ozone doses. The decline in the *N*-ethylethanimine oxide concentrations is likely associated with the formation of nitroethane. Nitrones have been suggested as intermediates during the transformation of secondary amines into nitroalkanes upon ozonation (Bailey et al., 1978; McCurry et al., 2016). Ethylamine, the other minor product, gradually increased with increasing ozone doses, persisting as a final product along with nitroethane. The nitrogen mass balance was well maintained up to an ozone dose of 100 μM but fell short by 10–24% for higher ozone doses, which is still reasonable compared to typical product studies. Attempts were made to identify *N,N*-diethylhydroxylamine as another possible transformation product by LC-MS/MS with the reference standard, but this compound was not detected (LOQ = 2.5 μM) at any ozone dose.

Reactive oxygen species. During the diethylamine-ozone reaction, 46% of $^1O_2$ and 26% of •OH were found relative to the consumed ozone (Table 2). The $^1O_2$ yield was higher than the reported value of 20% (Muñoz et al., 2001). However, a $^1O_2$ yield of 29% (Table S3) determined under similar conditions to the previous study (i.e., amine excess and without *t*-butanol) was closer to the reported value. The •OH yield was similar to a reported value of 28% for piperidine which contains a secondary amine moiety (Tekle-Röttering et al., 2016). The relatively high •OH yield found in the reaction of diethylamine with ozone does not match to the low formation of the corresponding dealkylated product, ethylamine. There seems another reaction pathway responsible for the excess of •OH apart from the electron transfer pathway of diethylamine leading to ethylamine (see section 3.2.3).

Reaction pathways. The diethylamine-ozone reaction can also be described by oxygen transfer and electron transfer pathways (Fig. 3). However, it entailed secondary ozone reactions with the primary transformation products, which makes the elucidation of the reaction mechanism more complicated than in the case of triethylamine. The yields of the identified transformation products at an ozone dose of 93 μM was calculated in analogy to the triethylamine-ozone reaction (transformation product formed/diethylamine abated): 26 ± 1% *N*-ethylethanimine oxide, 69 ± 13% nitroethane, and 8 ± 1% ethylamine. The total yield of the products with the oxygen addition (*N*-ethylethanimine oxide and nitroethane) was about 95%, outweighing the yield of the dealkylated amine (ethylamine, 8%). This suggests that the diethylamine-ozone reaction also predominantly undergoes an oxygen transfer pathway (step (a), Fig. 3). However, the reactive oxygen species yields were much higher than the yields of the corresponding transformation products: 186% for $^1O_2$ and 105% for •OH due to the little abatement of diethylamine (Δ[Diethylamine] = 23 μM). These high yields of reactive oxygen species as well as the high ozone stoichiometry (4 mol equivalents of ozone, Fig. 1b) and the highly oxidized product (nitroethane) imply secondary reactions of primary transformation products with ozone during the diethylamine-ozone reaction. It is hypothesized that *N,N*-diethylhydroxylamine might be a transient product. This is in analogy to *N*-oxides for the case of tertiary amines, as often suggested in other studies on the reaction of secondary amines with ozone (Benner and Ternes, 2009a; Tekle-Röttering et al., 2016; von Gunten, 2003). However, *N,N*-diethylhydroxylamine was not detected in our experiments. This contrasts a recent finding in the reaction of piperidine (a secondary amine) with ozone where a yield of 94% *N*-hydroxypiperidine was reported (Tekle-Röttering et al., 2016). The apparent disagreement can be explained by different pH conditions applied in the two studies. In the current study, the experiments were carried out at pH 7, where the apparent second-order rate constant for the reaction of *N,N*-diethylhydroxylamine with ozone is more than three orders of magnitude higher than the corresponding rate constant for diethylamine ($k_{obs,pH7}$, Table 1). Therefore, even if *N,N*-diethylhydroxylamine is formed as a primary transformation product during the diethylamine-ozone reaction, it would quickly react with ozone and be further oxidized, which would hinder its detection. In contrast, the experiment in the previous study was carried out at pH 11.5 where the kinetics for the reactions of ozone with piperidine and *N*-hydroxypiperidine only differ by a factor of two. Under these conditions and in excess of piperidine relative to ozone, *N*-hydroxypiperidine can be detected.

Quantum chemical computations. Quantum chemical computations were performed to calculate aqueous Gibbs free energy of reaction ($\Delta G_{aq,rxn}$) for the oxygen transfer and electron transfer pathways of the diethylamine-ozone reaction by assuming *N,N*-diethylhydroxylamine as the primary product of the oxygen transfer pathway (steps (a) and (b) in Fig. 3 and Reactions No. 1 and 2 in Table S4). The computations were made for the initial reaction step of each pathway in which diethylamine and ozone react to form *N,N*-diethylhydroxylamine and $^1O_2$ via an oxygen transfer (step (a), Fig. 3) or diethylaminyl radical ($(CH_3CH_2)N^\bullet$), proton (H^+), and ozonide radical anion ($O_3^{\bullet-}$) via electron transfer (step (b), Fig. 3). The $\Delta G_{aq,rxn}$ was compared to estimated values based on more accurate gas-phase reactions for the oxygen transfer pathway (Trogolo et al., 2019) or to reported one-electron standard reduction potentials for the electron transfer pathway (Jonsson et al., 1996; Wardman, 1989). The difference in $\Delta G_{aq,rxn}$ between the purely computed and the estimated values was <4 kcal mol^{-1} (details are given in Text S8 and Table S4), and the uncertainty of calculation should be in the same range. The results clearly show that the oxygen transfer pathway ($\Delta G_{aq,rxn} = -16.4$ kcal mol^{-1}) is thermodynamically more feasible than the electron transfer pathway ($\Delta G_{aq,rxn} = +9.3$ kcal mol^{-1}). This is another strong indication suggesting a predominance of an oxygen transfer pathway over an electron transfer pathway during the initial phase of the diethylamine-ozone reaction shown in Fig. 3.

3.2.3. *N,N*-diethylhydroxylamine-ozone reaction

Transformation products. To further investigate whether *N,N*-diethylhydroxylamine can be an intermediate of the diethylamine-ozone reaction, *N,N*-diethylhydroxylamine was treated with ozone separately and its transformation products (Fig. 1c) were compared with those of diethylamine (Fig. 1b). *N,N*-diethylhydroxylamine was indeed transformed to *N*-ethylethanimine oxide and nitroethane, the identical products as formed in the diethylamine-ozone reaction. *N*-ethylethanimine oxide was detected even for the samples without ozone (i.e., at 0 μM ozone), which was due to a spontaneous oxidation of hydroxylamines by oxygen to form nitrones (Johnson et al., 1956). Accordingly, the reaction time was reduced to 3–5 h to minimize the autoxidation. *N*-ethylethanimine oxide reached the maximum formation at 150 μM ozone where *N,N*-diethylhydroxylamine was completely abated, and decreased for higher ozone doses. The decrease in *N*-ethylethanimine oxide coincided with a gradual increase in nitroethane formation. Thus, the transformation reaction occurred in the sequence *N,N*-diethylhydroxylamine → *N*-ethylethanimine oxide → nitroethane. The mass balance of *N,N*-diethylhydroxylamine and the detected transformation products was within 82–116% for the entire range of ozone doses.

Reactive oxygen species. Similar yields of $^1O_2$ and •OH were determined for the reaction of *N,N*-diethylhydroxylamine with ozone (38% and 43%, Table 2). The $^1O_2$ yield increased to 50% at amine:ozone molar ratios >1 (Table S3). Under these conditions with amine in excess, *N,N*-diethylhydroxylamine was transformed into *N*-ethylethanimine oxide with 100% yield (0–150 μM ozone dose, Fig. 1c). Therefore, the initial phase of the *N,N*-

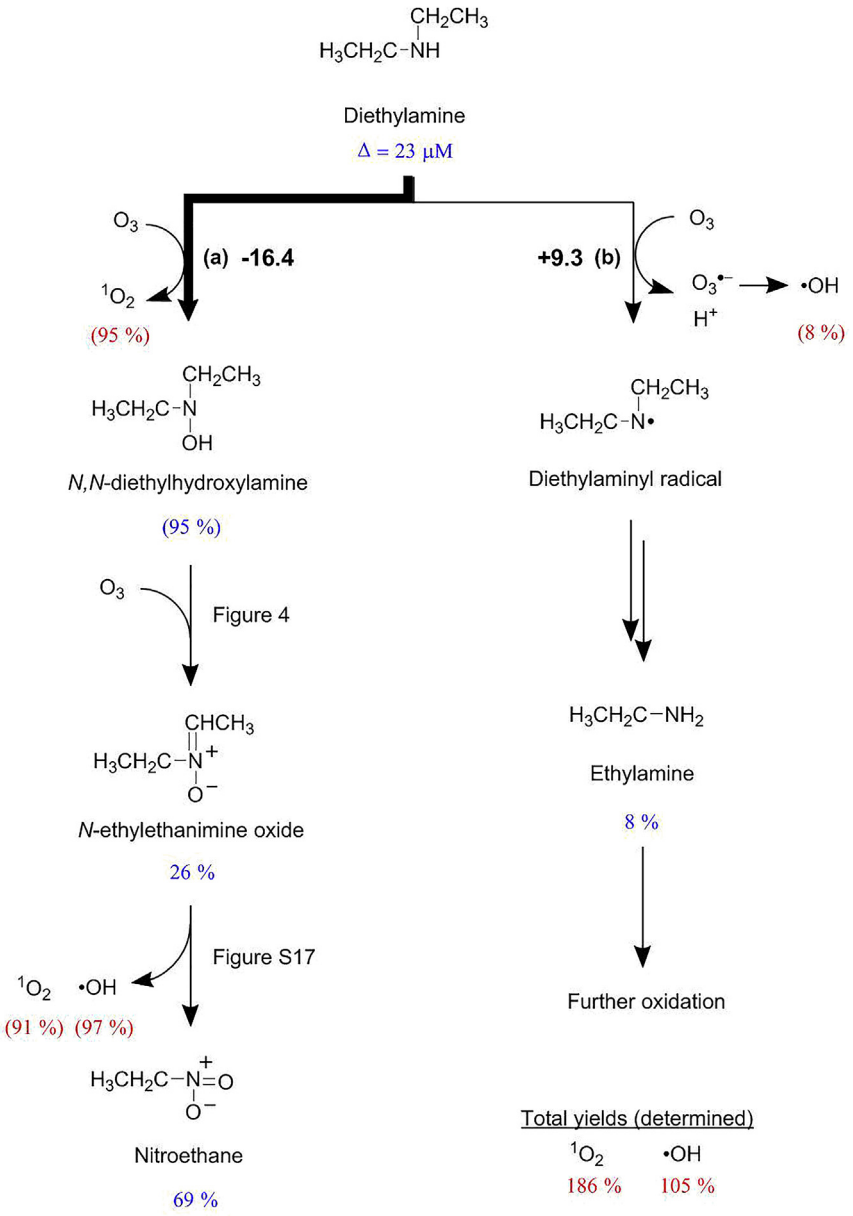

Fig. 3. Proposed mechanism for the reaction of diethylamine with ozone. Product yields (in %) were calculated by dividing the measured concentrations of the transformation products and the reactive oxygen species by the abated diethylamine (23 μM) at an ozone dose of 93 μM. The yield of *N,N*-diethylhydroxylamine in parenthesis is a theoretical yield based on the sum of the *N*-ethylethanimine oxide and nitroethane yields. The $^1O_2$ and •OH yields in parentheses are also theoretical yields based on the yields of the corresponding transformation products and the total $^1O_2$ and •OH yields determined for the diethylamine-ozone reaction (186% $^1O_2$ and 105% •OH). Bold numbers next to the reaction steps are calculated aqueous Gibbs free energies in kcal mol^{-1}. The bold arrow indicates the major pathway of the branched reaction.

diethylhydroxylamine-ozone reaction can be characterized by two distinct pathways yielding $^1O_2$ and •OH, which both led to the same product, *N*-ethylethanimine oxide. To investigate the secondary phase of the *N,N*-diethylhydroxylamine-ozone reaction where *N*-ethylethanimine oxide was transformed to nitroethane, we attempted to determine $^1O_2$ yields under ozone excess conditions (amine:ozone ≤ 1) and found the yields decreased as the specific ozone dose increased (Table S3). The low $^1O_2$ yields might be underestimated by the excess ozone which could quench $^1O_2$ formed during the *N,N*-diethylhydroxylamine-ozone reaction. The reaction of $^1O_2$ with ozone in the gas phase is known ($k = 2 \times 10^6$ M^{-1}s^{-1}) (Wayne and Pitts, 1969). However, currently little information is available for the quenching reaction in the aqueous phase.

Comparison of reactive oxygen species yields for diethylamine- and N,N-diethylhydroxylamine-ozone reactions. The reactive oxygen species yields of *N,N*-diethylhydroxylamine were compared to those of diethylamine to further examine the possibility of forming *N,N*-diethylhydroxylamine as a primary product of the diethylamine-ozone reaction. During the initial phase of the diethylamine-ozone reaction, 95% $^1O_2$ and 8% •OH would have been formed based on the yields of the corresponding transformation products, *N,N*-diethylhydroxylamine and ethylamine (steps (a) and (b), Fig. 3). As mentioned above, the total $^1O_2$ and •OH yields determined for the diethylamine-ozone reaction were 186% and 105%, respectively, thus the remaining 91% $^1O_2$ and 97% •OH would have resulted from secondary reactions of a primary transformation product, e.g., *N,N*-diethylhydroxylamine. The hypothetical $^1O_2$ and •OH yields for the

reaction of *N,N*-diethylhydroxylamine with ozone were estimated for the condition where *N*-ethylethanimine oxide and nitroethane were formed with 26% and 69% yields, respectively, as found in the diethylamine-ozone reaction. The ozone dose required for these specific product yields was approximately 270 μM (shown as a vertical line in Fig. 1c) for *N,N*-diethylhydroxylamine with an initial concentration of ~110 μM. For this ozone dose, *N,N*-diethylhydroxylamine was transformed to 31 μM N-ethylethanimine oxide (29% of the abated *N,N*-diethylhydroxylamine) and 80 μM nitroethane (72%) based on the simulated concentrations of the products (dotted lines in Fig. 1c; details on the simulation are discussed in section 3.2.4.). Converting the $^1O_2$ and •OH yields determined with regard to ozone (38% and 43%, Table 2) into the yields per abated *N,N*-diethylhydroxylamine with $[O_3] = 270\ \mu M$ and Δ[*N,N*-diethylhydroxylamine] = 110 μM resulted in 93% $^1O_2$ and 106% •OH. This agrees well with the aforementioned hypothetical yields, supporting *N,N*-diethylhydroxylamine as an intermediate of the diethylamine-ozone reaction.

Detailed reaction mechanisms. *N,N*-diethylhydroxylamine is a highly probable intermediate of the diethylamine-ozone reaction with a high theoretical yield of 95%. Therefore, it is important to understand how *N,N*-diethylhydroxylamine reacts with ozone to obtain a complete picture of the diethylamine-ozone reaction. Clearly, our results show that *N,N*-diethylhydroxylamine was quantitatively transformed into *N*-ethylethanimine oxide upon ozonation during the initial phase of the reaction (Fig. 1c). Based on the similarly high yields of $^1O_2$ and •OH from *N,N*-diethylhydroxylamine (38% for $^1O_2$ and 43% for •OH, Table 2), both oxygen transfer and electron transfer seem to play an important role in the initial transformation of *N,N*-diethylhydroxylamine into *N*-ethylethanimine oxide. The oxygen transfer pathway would proceed via a N^+-O-O-O^- adduct from an ozone attack on *N,N*-diethylhydroxylamine, which would then degrade into *N*-ethylethanimine oxide, $^1O_2$, and water (step (c), Fig. 4). The formation of a N^+-O-O-O^- adduct of a hydroxylamine was suggested by a study on the reaction of a primary amine with ozone in an organic solvent where a hydroxylamine was expected as a reaction intermediate, but with lack of experimental evidence (Bailey and Keller, 1968). In contrast, the electron transfer pathway would result in diethylnitroxide and ozonide radical anion ($O_3^{\bullet-}$) as primary products (step (d), Fig. 4). Electron transfer pathways forming nitroxide compounds were often suggested by other studies to describe the oxidation of hydroxylamines, e.g., with ozone as an oxidant in the gas phase (Olszyna and Heicklen, 1976), with molecular oxygen (Johnson et al., 1956), with $^1O_2$ (Encinas et al., 1987), and during photooxidation (Bilski et al., 1993). The formation of diethylnitroxide during the photooxidation of *N,N*-diethylhydroxylamine was experimentally confirmed by detecting the characteristic EPR signal (Bilski et al., 1993). Nitroxides containing α-hydrogens are susceptible to an attack by other radicals to form nitrones (Amar et al., 2015). Similarly, an α-hydrogen of diethylnitroxide can be abstracted by other radicals and transformed into *N*-ethylethanimine oxide (step (h), Fig. 4). Such radicals can be diethylnitroxide itself inducing a bimolecular reaction forming *N*-ethylethanimine oxide and *N,N*-diethylhydroxylamine (Adamic et al., 1970) or *t*-butanol derived peroxyl radicals (e.g., $C(CH_3)_2(OH)CH_2OO$•, hereafter referred to *t*-BuOO•) (Flyunt et al., 2003) likely present in the reaction system with high yields of •OH. Alternatively, diethylnitroxide can further react with ozone to form an aminyl radical (R_2N•), which will likely further react with ozone and cause an ozone-consuming chain reaction (steps (e) and (f), Fig. 4) (Sein et al., 2008; von Sonntag and von Gunten, 2012) or react also with *t*-BuOO• to decompose to 2-Methyl-1,2-propanediol and *N*-ethylethanimine oxide (step (i), Fig. 4). The ozone reaction kinetics of diethylnitroxide has not been determined yet. A similar compound with a nitroxide group but with no α-hydrogen, TEMPO, has a very high second-order rate constant for its reaction with ozone ($k_{O3} = 10^7\ M^{-1}s^{-1}$) (Muñoz and von Sonntag, 2000b). As the calculated $\Delta G_{aq,rxn}$ for the diethylnitroxide-ozone reaction (−16.7 kcal mol^{-1}, step (e) in Fig. 4) is slightly energetically less favorable than the reported $\Delta G_{aq,rxn}$ for the TEMPO-ozone reaction (−23.2 kcal mol^{-1}) (Naumov and von Sonntag, 2011), the kinetics of the diethylnitroxide-ozone reaction may be lower than $10^7\ M^{-1}s^{-1}$. In contrast, the kinetics of the reaction of diethylnitroxide with radical species vary widely from $8.0 \times 10^2\ M^{-1}s^{-1}$ (as the bimolecular reaction of diethylnitroxide) (Ingold et al., 1971) to $2.8 \times 10^7\ M^{-1}s^{-1}$ (as the reaction of TEMPO with *t*-BuOO•) (Goldstein and Samuni, 2007). Based on the available kinetic information, both reactions of diethylnitroxide with ozone and with radical seem probable, but we still propose that the radical reaction outcompetes the ozone reaction because of the following reasons: (1) Diethylaminyl radical resulted from the further ozone reaction would degrade into ethylamine via 1,2-H shift followed by a reaction with O_2 and hydrolysis (step (g), Fig. 4) (von Sonntag and von Gunten, 2012), which conflicts with the quantitative formation of *N*-ethylethanimine oxide as a primary product of the *N,N*-diethylhydroxylamine-ozone reaction (Fig. 1c); (2) A catalytic ozone consumption accompanied with the further ozone reactions (steps (e) and (f)) is inconsistent with the relatively low stoichiometry of about 1.5 mol equivalents of ozone for the initial phase of the *N,N*-diethylhydroxylamine-ozone reaction (Fig. 1c).

Quantum chemical computations. Quantum chemical computations of the $\Delta G_{aq,rxn}$ for the *N,N*-diethylhydroxylamine-ozone reaction were performed to test for an oxygen transfer or an electron transfer as the initial reaction step (steps (c) and (d) in Fig. 4 and Reactions No. 3 and 4 in Table S4). The results showed that the oxygen transfer pathway is significantly and thermodynamically more favorable than the electron transfer pathway (−61.2 kcal mol^{-1} for the oxygen transfer, −6.1 kcal mol^{-1} for the electron transfer). However, it is worth to note that the electron transfer pathway is exergonic for the *N,N*-diethylhydroxylamine-ozone reaction, in contrast to the diethylamine-ozone reaction where the $\Delta G_{aq,rxn}$ of the electron transfer pathway is +9.3 kcal mol^{-1}. This implies that *N,N*-diethylhydroxylamine-ozone reaction may have a higher probability to undergo an electron transfer pathway than the diethylamine-ozone reaction, which is confirmed by similar $^1O_2$ and •OH yields.

3.2.4. *N*-ethylethanimine oxide-ozone reaction

Transformation products. The last piece of information needed to understand the diethylamine-ozone reaction is the transformation of *N*-ethylethanimine oxide to nitroethane. An ozonation experiment was carried out for *N*-ethylethanimine oxide using the synthesized stock described in Text S1 to investigate if it could be a transient product with a high yield of nitroethane. Nitroethane was indeed identified as a major product with a 73% yield based on the abated *N*-ethylethanimine oxide at 300 μM ozone (Fig. S13). However, there were a few distinguishing features observed in this separate ozonation experiment with *N*-ethylethanimine oxide as a starting material, compared to the *N,N*-diethylhydroxylamine-ozone reaction (Fig. 1c) where *N*-ethylethanimine oxide was formed as an intermediate and further degraded. We assume the difference was caused by a spontaneous dimerization of *N*-ethylethanimine oxide (Ali et al., 2010; Roca-López et al., 2014), which contaminated the primary stock solution used in the separate ozonation experiment and affected the reaction of *N*-ethylethanimine oxide with ozone (Text S7). Therefore, for further discussions regarding *N*-ethylethanimine oxide, we rely on the result from the *N,N*-diethylhydroxylamine-ozone reaction at high ozone doses (100–300 μM). Under these conditions, *N*-ethylethanimine

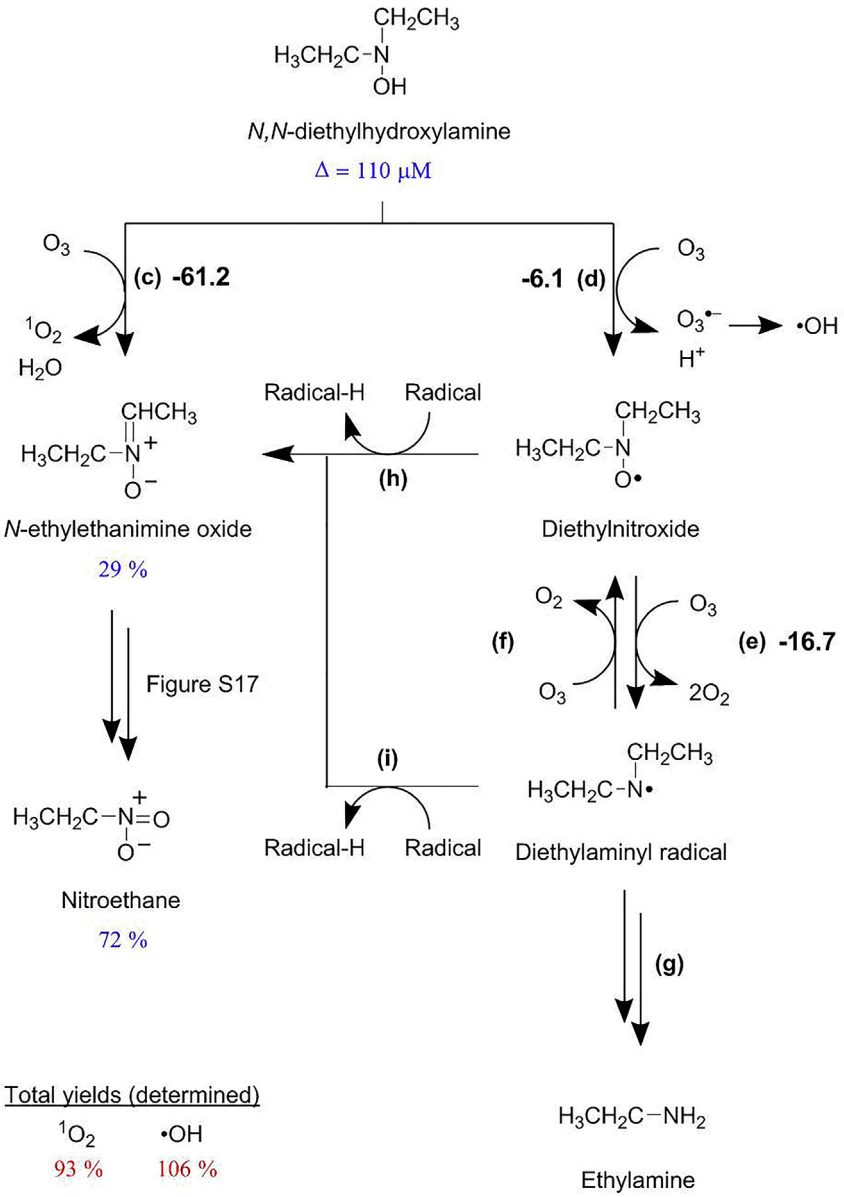

Fig. 4. Proposed mechanism for the reaction of *N,N*-diethylhydroxylamine and *N*-ethylethanimine oxide with ozone. Product yields (in %) were calculated by dividing the simulated concentrations of the transformation products and the measured concentrations of reactive oxygen species by the abated *N,N*-diethylhydroxylamine (110 μM) at an ozone dose of 270 μM. Bold numbers next to the reaction steps are calculated aqueous Gibbs free energies in kcal mol^{-1}. For discussion of reactions (c)–(i) see text.

oxide is formed *in situ* and not affected by dimerization. Because of these experimental shortcomings, also the results of the reactive oxygen species in the experiments with *N*-ethylethanimine oxide should be interpreted cautiously by taking the presence of a dimer into account.

Kinetic simulation: N,N-diethylhydroxylamine- and N-ethylethanimine oxide-ozone reactions. Based on the information obtained so far, we performed kinetic simulations to describe the evolution of *N,N*-diethylhydroxylamine, *N*-ethylethanimine oxide, and nitroethane during the *N,N*-diethylhydroxylamine-ozone reaction by using the Kintecus software (www.kintecus.com) (Ianni, 2017) (Table S5 and Fig. 1c, dotted lines). The kinetic model contained the initial transformation reaction of *N,N*-diethylhydroxylamine to *N*-ethylethanimine oxide, diethylnitroxide, and an unknown radical species, X, via oxygen transfer and electron transfer pathways with a 1:1 branching ratio. X is a radical species (e.g., *t*-BuOO•) derived from the scavenging reaction of •OH with *t*-butanol, formed by the electron transfer reaction along with diethylnitroxide. The 1:1 ratio was selected based on the similar yields of $^1O_2$ and •OH, the indicators of oxygen transfer and electron transfer, for the conditions where *N,N*-diethylhydroxylamine was in molar excess of ozone (i.e., amine:ozone > 1, Table S3 and Fig. S12). The ensuing products of electron transfer, diethylnitroxide and X, react with each other and subsequently form *N*-ethylethanimine oxide. Additionally, the autoxidation of *N,N*-diethylhydroxylamine was included assuming oxygen saturation at 20 °C ([O_2 (aq)] ~ 9 mg/l). A bimolecular reaction of diethylnitroxide to form *N,N*-diethylhydroxylamine and *N*-ethylethanimine oxide was also included to describe the decay of diethylnitroxide under conditions without ozone (0 μM ozone). Lastly, two more reaction steps were added to describe the transformation of *N*-ethylethanimine oxide into nitroethane via an unknown intermediate, Y, which was assumed to react very fast with ozone (assumed $k_{obs,pH7} = 1 \times 10^6\ M^{-1}s^{-1}$) to form nitroethane. The simulation results shown in Fig. 1c (dotted lines) are in reasonable

agreements with the experimental findings of the *N,N*-diethylhydroxylamine-ozone reaction which formed *N*-ethylethanimine oxide and nitroethane in a sequential order.

Detailed reaction mechanisms. Compounds containing C-N double bonds like nitrones and oximes typically form *C*-nitroso compounds upon ozonation according to the studies conducted in organic solvents (Bailey et al., 1978; Erickson et al., 1969; Riebel et al., 1960). Similarly, *N*-ethylethanimine oxide could react with ozone to form nitrosoethane which would be further oxidized by ozone to form nitroethane (steps (j) – (k), Fig. S17). However, as the nitroso moiety is a strong electron-withdrawing group, nitrosoethane cannot be the intermediate Y hypothesized to be highly reactive to ozone in the kinetic simulation. This was tested by a kinetic simulation substituting nitrosoethane for Y and using the same kinetic model but with a different $k_{obs,pH7}$ of the reaction No. 6 set at $1.0 \times 10^2\ M^{-1}s^{-1}$ instead of $1.0 \times 10^6\ M^{-1}s^{-1}$ (Table S6). The new model with nitrosoethane as an intermediate did not perform as well as the previous one, featuring a lower ozone stoichiometry of the abatement of *N*-ethylethanimine oxide than the measured value (Fig. S16b). Another possible mechanism of the *N*-ethylethanimine oxide-ozone reaction can be a Criegee-type mechanism forming an ozonide via a cycloaddition of ozone to the C-N double bond (step (l), Fig. S17) (Criegee, 1975; Dowideit and von Sonntag, 1998). The ozonide would dissociate into nitroethane and a peroxide intermediate. The latter would subsequently react with water to form acetaldehyde and hydrogen peroxide (Criegee and Wenner, 1949; Criegee, 1975). To test this hypothesis, the formation of hydrogen peroxide was determined in ozonated *N*-ethylethanimine oxide samples. The *N*-ethylethanimine oxide solution was prepared *in situ* by oxidizing ~100 μM N,*N*-diethylhydroxylamine with 180 μM ozone to ensure all *N,N*-diethylhydroxylamine was converted to *N*-ethylethanimine oxide. Thereafter, 100 μM ozone was added to the *N*-ethylethanimine oxide solution. The concentrations of hydrogen peroxide in the *N*-ethylethanimine oxide solution before and after the ozone addition remained the same (16 ± 4 μM for both). This confirms that hydrogen peroxide was not formed during the reaction of *N*-ethylethanimine oxide with ozone and thus, makes the Criegee-type mechanism very unlikely. The other hypothesis is an electron transfer pathway forming a *N*-ethylethanimine oxide radical cation and an ozonide radical anion (step (m), Fig. S17). This pathway can explain the possibly high •OH yield of *N*-ethylethanimine oxide (43%, Table 2). One-electron oxidation of nitrones has been postulated as an alternative spin trapping mechanism when nitrones were used as radical spin traps (Eberson, 1994; Zubarev and Brede, 1994). The resulting nitrone radical cations were detected experimentally (Zubarev and Brede, 1994). However, little is known whether a similar pathway can be applied to the ozone reaction and how the radical cation further degrades into nitroethane.

Quantum chemical computations. The hypothesized mechanisms of the *N*-ethylethanimine oxide-ozone reaction (steps (j) and (l), Fig. S17) were examined by calculating $\Delta G_{aq,rxn}$ of the reactions. The $\Delta G_{aq,rxn}$ of the reaction step (m) could not be calculated because of an unreliable result of the computation of the *N*-ethylethanimine oxide radical cation at the CCSD(T)/jul-cc-pVTZ level, resulting in T1 diagnostic > 0.03 (Lee and Taylor, 1989). Besides the ozone reactions, the hydrolysis of *N*-ethylethanimine oxide forming *N*-ethylhydroxylamine and acetaldehyde (step (n), Fig. S17), suggested by an earlier study (von Gunten, 2003), was also examined because this could compete with the further reaction of *N*-ethylethanimine oxide with ozone. The calculations show that the further reactions with ozone are thermodynamically more feasible than the hydrolysis which is endergonic (−40.8 kcal mol^{-1} and −70.8 kcal mol^{-1} for the ozone reactions and +8.4 kcal mol^{-1} for hydrolysis, steps (j), (l), and (n) in Fig. S17 and Reaction No. 6–8 in Table S4). However, despite the thermodynamic feasibility of the reaction steps (j) and (l), neither of them were justified by the experimental findings as discussed above. This demonstrates that the results from quantum chemical computations must be interpreted cautiously and considered as supplementary information to experimental findings.

Kinetic simulation: diethylamine-ozone reaction. Finally, a kinetic simulation for the diethylamine-ozone reaction was carried out (Table S7 and Fig. 1b, dotted lines). The kinetic model included the initial transformation reaction of diethylamine to *N,N*-diethylhydroxylamine and diethylaminyl radical with a 9:1 branching ratio based on the product yields. The follow-up reaction steps were applied as in the model for the *N,N*-diethylhydroxylamine-ozone reaction (Table S5). The trends for the abatement of diethylamine and the evolution of the various transformation products were well described. However, the simulated concentrations of the final products (nitroethane and ethylamine) at 300 μM ozone dose were about 50% higher than the measured concentrations (Fig. 1b). For such a complex reaction system, this is a reasonable outcome.

3.2.5. Ethylamine-ozone reaction

Transformation products. About 5.5 molar equivalents of ozone were required for a complete abatement of ethylamine (Fig. 1d). Nitroethane was the major product with close to 100% yields at all ozone doses, resulting in a very good mass balance. Therefore, only very limited additional products are expected from the ethylamine-ozone reaction. The high yield of nitroethane observed in the ethylamine-ozone reaction is in agreement with a recent study that found 100% nitromethane from methylamine with a molar ozone:methylamine ratio of 12 (McCurry et al., 2016). However, these results disagree with previous studies, where nitrate was detected as a final product from the ozone reactions of ammonia (Hoigné and Bader, 1978) and amino acids containing a primary amine moiety (Berger et al., 1999; de Vera et al., 2017; Le Lacheur and Glaze, 1996). In the current study, only traces of nitrite and nitrate were detected from ethylamine over the entire range of ozone doses (<1%, not shown in Fig. 1d). Additional ozonation experiments were carried out with ozone:ethylamine ratios of 20, but still only about 10% nitrate was detected. This is far smaller than previously reported nitrate yields from amino acids (glycine and serine) of 85–90% with molar ozone:model compound ratios of 5–20 (Berger et al., 1999; de Vera et al., 2017; Le Lacheur and Glaze, 1996). The discrepancy may be due to the presence of a carboxylic group in the amino acids, which alters the reaction pathway to favor nitrate rather than nitroalkanes as final products (see the section "*primary amines vs amino acids*" below). Ammonia, a dealkylated product from ethylamine, is unlikely to be formed, because the nitrogen mass balance was completed by nitroethane alone. No ammonia formation was also reported in the oxidation of glycine by ozone in presence of a radical scavenger (Berger et al., 1999).

Reactive oxygen species. Similar yields of $^1O_2$ and •OH were determined for the ethylamine-ozone reaction (27% and 33% relative to the consumed ozone for $^1O_2$ and •OH, respectively, Table 2). The $^1O_2$ yield was slightly higher than the previously reported value of 17% (Muñoz et al., 2001). The •OH yield was similar to the yield from glycine which contains a primary amine moiety (de Vera et al., 2017). Similar to the diethylamine-ozone reaction, the significant yield of •OH seems to be a result of secondary ozone reactions of primary transformation products rather than from the initial phase of the ethylamine-ozone reaction.

Reaction pathways. The ethylamine-ozone reaction can be understood similarly to the diethylamine-ozone reaction as it was characterized by the same features: high ozone stoichiometry, the formation of a highly oxidized product (nitroethane), and high yields of reactive oxygen species per abated amine (Fig. 5). The yields of nitroethane and reactive oxygen species ($^1O_2$ and •OH) at

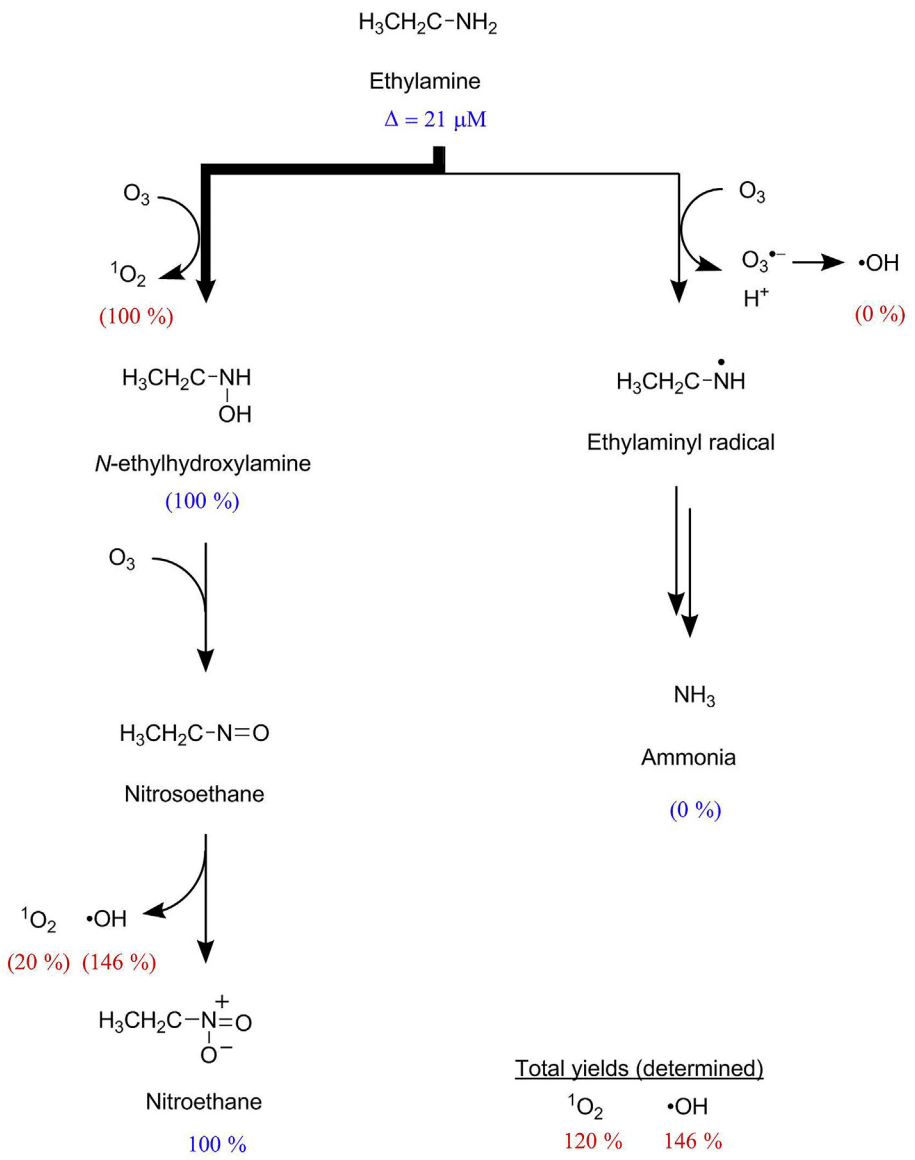

Fig. 5. Proposed mechanism for the reaction of ethylamine with ozone. Product yields (in %) were calculated by dividing the measured concentrations of the transformation products and the reactive oxygen species by the abated ethylamine (21 μM) at an ozone dose of 93 μM. The yield of *N*-ethylhydroxylamine in parenthesis is a theoretical yield based on the nitroethane yield. The $^1O_2$ and •OH yields in parentheses are also theoretical yields based on the yields of the corresponding transformation products and the total $^1O_2$ and •OH yields determined for the ethylamine-ozone reaction (120% $^1O_2$ and 146% •OH). The bold arrow indicates the major pathway of the branched reaction.

93 μM ozone are 100%, 120% and 146%, respectively, where Δ[Ethylamine] = 21 μM. The ethylamine-ozone reaction mainly underwent oxygen transfer reaction based on a 100% yield of nitroethane. Accordingly, *N*-ethylhydroxylamine and $^1O_2$, the primary transformation product and the reactive oxygen species of the oxygen transfer pathway, would be formed with 100% theoretical yields. The remaining $^1O_2$ and •OH yields (20% and 146%) should be associated with secondary reactions leading to nitroethane. However, considering the high ozone stoichiometry of 5.5 mol equivalents of ozone (or 550% ozone in relation to abated ethylamine), the total reactive oxygen species yield (266%) was too low. Thus, more reactive oxygen species (e.g., $^1O_2$ and •OH which might have been underestimated or superoxide radical and hydrogen peroxide which have not been determined) seems to be involved in the secondary reactions than what was actually measured.

Detailed reaction mechanisms. *N*-ethylhydroxylamine is expected as a primary transformation product via oxygen transfer in analogy to *N,N*-diethylhydroxylamine of the diethylamine-ozone reaction. Similar to *N,N*-diethylhydroxylamine, *N*-ethylhydroxylamine ($k_{obs,pH\ 7}$ ~10^5 $M^{-1}s^{-1}$, Table 1) reacts much faster with ozone than the parent amine, wherefore, it was not detectable and the formation of further oxidized products can be expected. During the further reaction of *N*-ethylhydroxylamine with ozone, a dihydroxylamine intermediate would be formed (Fig. S18a), as suggested by studies on ozone reactions of primary amines in organic solvents (Bachman and Strawn, 1968; Bailey and Keller, 1968). The dihydroxylamine intermediate would degrade to nitrosoethane or acetaldoxime by releasing water. Neither of these products were identified due to the lack of reference standards or an applicable analytical method. Nitroso compounds and oximes are tautomers of each other and oximes are known to be the more stable forms (Long et al., 2001). Although the tautomeric equilibrium would favor the formation of acetaldoxime, nitrosoethane still seems a more probable product based on the predominant formation of

nitroethane. If acetaldoxime was formed, the major product would have been nitrate, since acetaldoxime is hydrolyzed to hydroxylamine which can react fast with ozone ($k_{O3} = 2.1 \times 10^4\ M^{-1}s^{-1}$ for hydroxylamine) (Hoigné et al., 1985) to nitrate. Therefore, the high yield of nitroethane supports nitrosoethane as a precursor rather than acetaldoxime.

Primary amines vs amino acids. The different nitrate yields for primary amines and amino acids upon ozonation may be related to the secondary reaction pathways involving dihydroxylamines, nitroso compounds, or oximes as intermediates. Ethylamine and glycine, differing only by a substituent of the α-carbon (methyl for ethylamine and carboxyl for glycine), are compared in detail in Fig. S18. The nitrate yields per abated amines under ozone-excess conditions (≥5 molar equivalent ozone) were 10% for ethylamine (determined in this study) and 90% for glycine (Berger et al., 1999). To explain the high nitrate yield from glycine, we hypothesized that the nitroso intermediate of glycine can not only degrade into nitroacetic acid (McCurry et al., 2016), but also produce nitrate as a final product similar to the oxime counterpart (Fig. S18b). This is because the carboxyl group in the nitroso intermediate of glycine can decarboxylate, leaving formaldehyde oxime as the other product. The resulting formaldehyde oxime would be transformed into hydroxylamine and then nitrate in the same manner as the other oxime intermediates. The same decarboxylation mechanism was suggested for oxidation of amino acids by dimethyldioxirane, an electrophilic compound, for which the corresponding oximes and the carboxylic acids (resulted from further decomposition of the oximes) were found as major products (Paradkar et al., 1995). In comparison, the reactions of primary amines with dimethyldioxirane produce nitro compounds with high yields (Murray et al., 1986). Alternatively, it can be hypothesized that the carboxyl group can withdraw electron density from the neighboring α-carbon and render the α-carbon more acidic and thus prone to lose a proton. As a result, the oxime intermediate may be formed more efficiently than the nitroso counterpart. The deprotonation of the α-carbon of amino acids has been accepted as a key step of the racemization of amino acids (Smith and Sivakua, 1983). The pK_a of the α-carbon of glycine in the zwitterion form was determined to be 29 in aqueous solution (Rios et al., 2000). With the two additional hydroxyl groups, the α-carbon of the dihydroxylamine intermediate of glycine may be characterized by a much lower pK_a. Overall, the involvement of the oxime intermediates, either derived from dihydroxylamine intermediate or from nitroso intermediate, seems a decisive factor to explain the high nitrate yield from amino acids in comparison to primary amines.

3.2.6. Reaction mechanisms of aliphatic amines with ozone

Based on the findings of this study as well as available information in literature (Bailey et al., 1978; Bailey and Keller, 1968; Benner and Ternes, 2009b; Berger et al., 1999; Borowska et al., 2016; de Vera et al., 2017; Muñoz and von Sonntag, 2000a; Tekle-Röttering et al., 2016; Zimmermann et al., 2012), the reactions of aliphatic primary, secondary, and tertiary amines with ozone are summarized in Fig. 6. Our study revealed that all amines were predominantly transformed into products containing nitrogen-oxygen bonds, i.e., triethylamine *N*-oxide or nitroethane (64–100% of the transformed parent amines at the highest applied ozone dose). Dealkylated products were formed only as small fractions of the transformed parent compounds (0–9%).

3.3. Practical implications

Nitroethane was detected as a final product in all tested amine-ozone reactions. The yield was considerable for almost all amines (>60% for diethylamine, ethylamine, *N,N*-diethylhydroxylamine, and *N*-ethylethanimine oxide) except for triethylamine (9%). Short-chain aliphatic amines such as methylamine, dimethylamine, ethylamine, and diethylamine are typically present up to 0.1 μM in surface waters and up to 5 μM in wastewater effluents (Ábalos et al., 1999; Chen et al., 2014; Hwang et al., 1995; Mitch and Sedlak, 2004; Sacher et al., 1997). Considering the amount of aliphatic amines formed as breakdown products from more complex organic compounds, the total concentration of the short-chain nitroalkanes derived from aliphatic amines can be higher than 5 μM after ozonation. The reactivity of nitroalkanes towards ozone is expected to be low based on the low second-order ozone rate constant of nitroethane determined in this study ($k = 3.4\ M^{-1}s^{-1}$, Table 1). Thus, once formed, nitroalkanes would not be further transformed by ozone but persistent in water as they are not easily hydrolyzed nor biodegradable (USEPA, 1985). Moreover, the volatility of short-chain nitroalkanes is in the same range as trihalomethanes, known disinfection byproducts in chlorinated waters, based on the comparable Henry's constants ($2.9 \times 10^{-5} - 1.2 \times 10^{-4}$ atm m^3 mol^{-1} for nitroalkanes and $4.4 \times 10^{-4} - 7.8 \times 10^{-3}$ atm m^3 mol^{-1} for trihalomethanes) (Sander, 2015). Therefore, exposures to nitroalkanes could occur via inhalation or dermal adsorption during showering and bathing, similarly to trihalomethanes (WHO, 2005). The short-chain nitroalkanes such as nitromethane, nitroethane, 1-nitropropane, and 2-nitropropane are widely used as industrial solvents, building blocks for chemical syntheses, and fuels in combustion engines (Markofsky, 2011). Accordingly, studies on the toxicity of the nitroalkanes have mostly been conducted in the context of occupational exposures at workplaces where the nitroalkanes are used in high concentrations. Exposure to high levels of nitroalkanes causes acute and short-term toxicity (nitrite-induced methemoglobinemia) typically with little lingering effects. Such high levels of nitroalkanes are unlikely to be formed during water and wastewater treatment. Some nitroalkanes (nitromethane and 2-nitropropane) are reasonably anticipated to be human carcinogens (National Toxicology Program, 2016) and effects of long-term exposure to them have been of great concern. Therefore, further information is needed on the occurrence of nitroalkanes during ozonation, especially in the context of wastewater-impacted source waters and water reuse systems, where relatively high concentrations of aliphatic amines are expected in the dissolved organic matter.

4. Conclusion

- All amines predominantly underwent oxygen transfer reactions as initial ozone reaction pathways to form major products containing nitrogen-oxygen bonds, e.g., triethylamine *N*-oxide (triethylamine) or nitroethane (diethylamine and ethylamine). The yields of the major products were 69–100% per abated amines with one molar equivalent of ozone (93 μM). *N*-dealkylated products were additionally identified for triethylamine and diethylamine, but the yields were lower than 10%. Good nitrogen mass balances were achieved for all amine-ozone reactions (>70%).
- *N,N*-diethylhydroxylamine, a potential intermediate of the diethylamine-ozone reaction, escaped from our detection because of its high reactivity towards ozone in comparison to the ozone reactivity of diethylamine. However, the measurements of reactive oxygen species ($^1O_2$ and •OH), quantum chemical computations, and kinetic simulations support the possibility of forming *N,N*-diethylhydroxylamine during the diethylamine-ozone reaction.
- Different from the triethylamine-ozone reaction, the reactions of diethylamine and ethylamine with ozone were characterized by the high ozone molar stoichiometry (ozone:amine ≥ 4),

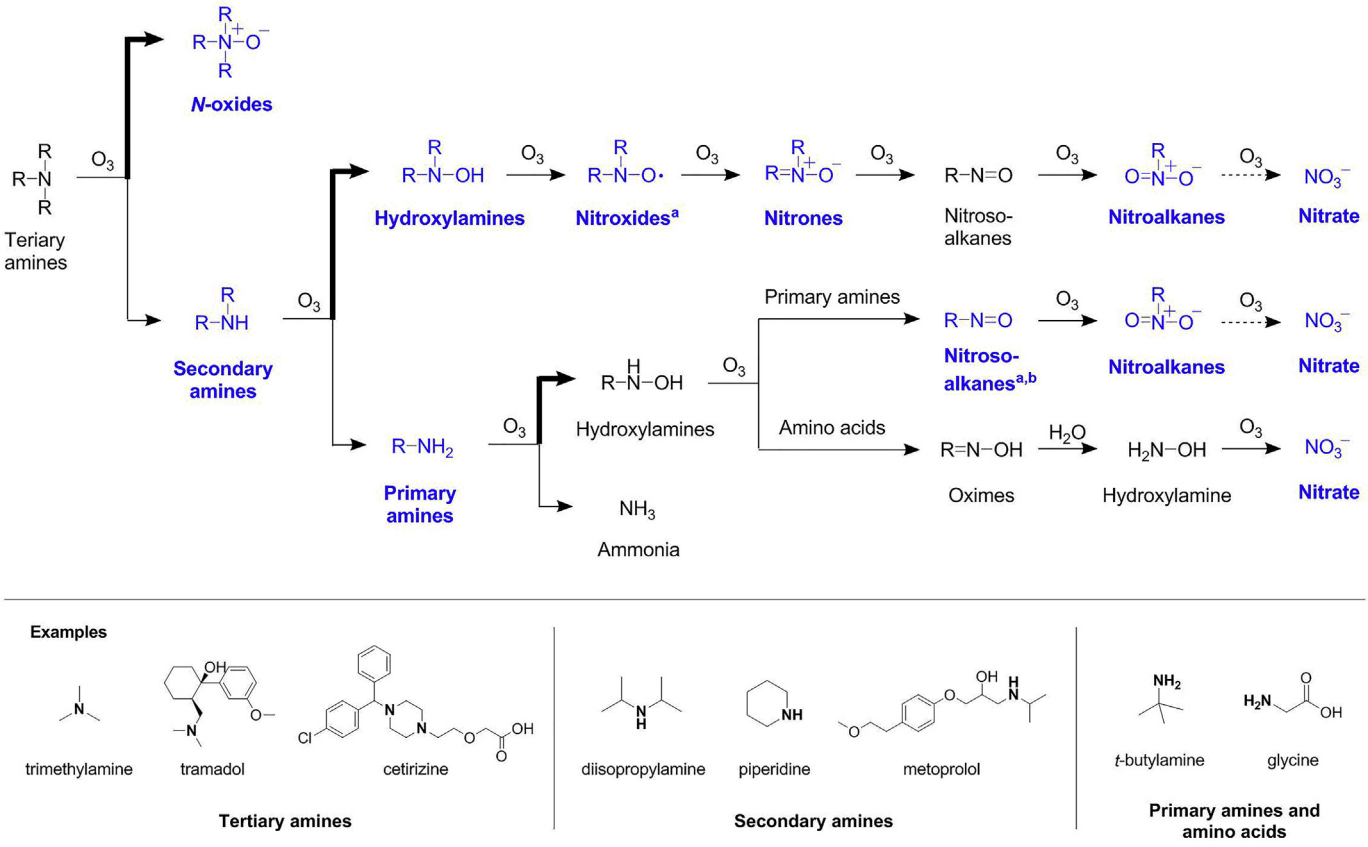

Fig. 6. Summary of the reactions of aliphatic primary, secondary, and tertiary amines with ozone in aqueous solution based on this and other studies (both acyclic and saturated heterocyclic amines as shown in the examples) (Bailey et al., 1978; Bailey and Keller, 1968; Benner and Ternes, 2009b; Berger et al., 1999; Borowska et al., 2016; de Vera et al., 2017; Muñoz and von Sonntag, 2000a; Tekle-Röttering et al., 2016; Zimmermann et al., 2012). Bold arrows indicate the dominant pathway. Identified transformation products are highlighted in blue and in bold. [a]Detected only in organic solvent (Bailey et al., 1978). [b]Indirectly confirmed based on a change in color of the solution (Bailey and Keller, 1968). (For interpretation of the references to color in this figure legend, the reader is referred to the Web version of this article.)

which resulted in the formation of a highly oxidized product (nitroethane) and an excess formation of $^1O_2$ and •OH.

- The high yields of nitroethane from diethylamine- and ethylamine-ozone reactions determined in this study imply significant formation of nitroalkanes during ozonation especially for waters containing high levels of dissolved organic nitrogen (e.g., wastewater-impacted sources waters). Further efforts are required to understand the occurrence of nitroalkanes and their impact on the receiving aquatic environment and human health.

Declaration of interests

The authors declare that they have no known competing financial interests or personal relationships that could have appeared to influence the work reported in this paper.

Acknowledgment

We thank Elisabeth Salhi for her support in the laboratory, Paul Erickson and Kris McNeill for their advice on the singlet oxygen measurement, Marc Bourgin, Philipp Longree and Jakov Bolotin for their support with MS measurements, Peter Tentscher for his help on quantum chemical computations, and Samuel Derrer for the synthesis of *N*-ethylethanimine oxide.

Appendix A. Supplementary data

Supplementary data to this article can be found online at https://doi.org/10.1016/j.watres.2019.03.089.

References

Ábalos, M., Bayona, J.M., Ventura, F., 1999. Development of a solid-phase microextraction GC-NPD procedure for the determination of free volatile amines in wastewater and sewage-polluted waters. Anal. Chem. 71, 3531–3537. https://doi.org/10.1021/ac990197h.

Adamic, K., Bowman, D.F., Ingold, K.U., 1970. Self-reaction of diethylnitroxide radicals. J. Am. Chem. Soc. 92, 1093–1094. https://doi.org/10.1021/ja00707a076.

Ali, S.A., AlSbaiee, A., Wazeer, M.I.M., 2010. Conformational analysis and inversion process in some perhydrodipyrido[1,2-b;1′2′-e]-1,4,2,5- dioxadiazines. J. Phys. Org. Chem. 23, 488–496. https://doi.org/10.1002/poc.1627.

Amar, M., Bar, S., Iron, M.A., Toledo, H., Tumanskii, B., Shimon, L.J.W., Botoshansky, M., Fridman, N., Szpilman, A.M., 2015. Design concept for α-hydrogen-substituted nitroxides. Nat. Commun. 6, 6070. https://doi.org/10.1038/ncomms7070.

Andrzejewski, P., Kasprzyk-Hordern, B., Nawrocki, J., 2008. N-nitrosodimethylamine (NDMA) formation during ozonation of dimethylamine-containing waters. Water Res. 42, 863–870. https://doi.org/10.1016/j.watres.2007.08.032.

Bachman, G.B., Strawn, K.G., 1968. Ozone oxidation of primary amines to nitroalkanes. J. Org. Chem. 33, 313–315. https://doi.org/10.1021/jo01265a062.

Bader, H., Hoigné, J., 1981. Determination of ozone in water by the indigo method. Water Res. 15, 449–456.

Bailey, P.S., Keller, J.E., 1968. Ozonation of amines. III. tert-Butylamine. J. Org. Chem. 33, 2680–2684.

Bailey, P.S., Southwick, L.M., Carter Jr., T.P., 1978. Ozonation of nucleophiles. 8. Secondary amines. J. Org. Chem. 43, 2657–2662.

Becke, A.D., 1993. Density-functional thermochemistry. III. The role of exact

exchange. J. Chem. Phys. 98, 5648–5652. https://doi.org/10.1063/1.464913.
Benner, J., Ternes, T.A., 2009a. Ozonation of propranolol: formation of oxidation products. Environ. Sci. Technol. 43, 5086–5093. https://doi.org/10.1021/es900282c.
Benner, J., Ternes, T.A., 2009b. Ozonation of metoprolol: elucidation of oxidation pathways and major oxidation products. Environ. Sci. Technol. 43, 5472–5480. https://doi.org/10.1021/es900280e.
Berger, P., Karpel Vel Leitner, N., Doré, M., Legube, B., 1999. Ozone and hydroxyl radicals induced oxidation of glycine. Water Res. 33, 433–441. https://doi.org/10.1016/S0043-1354(98)00230-9.
Bilski, P., Motten, A.G., Bilska, M., Chignell, C.F., 1993. The photooxidation of diethylhydroxylamine by rose Bengal in micellar and nonmicellar aqueous solutions. Photochem. Photobiol. 58, 11–18. https://doi.org/10.1111/j.1751-1097.1993.tb04896.x.
Bond, T., Huang, J., Templeton, M.R., Graham, N., 2011. Occurrence and control of nitrogenous disinfection by-products in drinking water – a review. Water Res. 45, 4341–4354. https://doi.org/10.1016/j.watres.2011.05.034.
Bond, T., Templeton, M.R., Graham, N., 2012. Precursors of nitrogenous disinfection by-products in drinking water––A critical review and analysis. J. Hazard Mater. 1–16, 235–236. https://doi.org/10.1016/j.jhazmat.2012.07.017.
Borowska, E., Bourgin, M., Hollender, J., Kienle, C., McArdell, C.S., von Gunten, U., 2016. Oxidation of cetirizine, fexofenadine and hydrochlorothiazide during ozonation: kinetics and formation of transformation products. Water Res. 94, 350–362. https://doi.org/10.1016/j.watres.2016.02.020.
Bourgin, M., Beck, B., Boehler, M., Borowska, E., Fleiner, J., Salhi, E., Teichler, R., von Gunten, U., Siegrist, H., McArdell, C.S., 2018. Evaluation of a full-scale wastewater treatment plant upgraded with ozonation and biological post-treatments: abatement of micropollutants, formation of transformation products and oxidation by-products. Water Res. 129, 486–498. https://doi.org/10.1016/j.watres.2017.10.036.
Chen, G., Liu, J., Liu, M., Li, G., Sun, Z., Zhang, S., Song, C., Wang, H., Suo, Y., You, J., 2014. Sensitive, accurate and rapid detection of trace aliphatic amines in environmental samples with ultrasonic-assisted derivatization microextraction using a new fluorescent reagent for high performance liquid chromatography. J. Chromatogr. A 1352, 8–19. https://doi.org/10.1016/j.chroma.2014.05.061.
Criegee, R., Wenner, G., 1949. Die Ozonisierung des 9,10-Oktalins. Justus Liebigs Ann. Chem. 564, 9–15. https://doi.org/10.1002/jlac.19495640103.
Criegee, R., 1975. Mechanism of ozonolysis. Angew. Chem. Int. Ed. 14, 745–752.
de Vera, G.A., Gernjak, W., Weinberg, H., Farré, M.J., Keller, J., von Gunten, U., 2017. Kinetics and mechanisms of nitrate and ammonium formation during ozonation of dissolved organic nitrogen. Water Res. 108, 451–461. https://doi.org/10.1016/j.watres.2016.10.021.
Dodd, M.C., Kohler, H.-P.E., von Gunten, U., 2009. Oxidation of antibacterial compounds by ozone and hydroxyl radical: elimination of biological activity during aqueous ozonation processes. Environ. Sci. Technol. 43, 2498–2504. https://doi.org/10.1021/es8025424.
Dowideit, P., von Sonntag, C., 1998. Reaction of ozone with ethene and its methyl- and chlorine-substituted derivatives in aqueous solution. Environ. Sci. Technol. 32, 1112–1119.
Eberson, L., 1994. Inverted spin trapping. Part 111." further studies on the chemical and photochemical oxidation of spin traps in the presence of nucleophiles. J. Chem. Soc. Perkin Trans. 2 (0), 171–176.
Eggen, R.I.L., Hollender, J., Joss, A., Schärer, M., Stamm, C., 2014. Reducing the discharge of micropollutants in the aquatic environment: the benefits of upgrading wastewater treatment plants. Environ. Sci. Technol. 48, 7683–7689. https://doi.org/10.1021/es500907n.
Encinas, M.V., Lemp, E., Lissi, E.A., 1987. Interaction of singlet oxygen [O2(1Δ)] with aliphatic amines and hydroxylamines. J. Chem. Soc., Perkin Trans. 2 0, 1125–1127. https://doi.org/10.1039/P29870001125.
Erickson, R.E., Andrulis Jr., P.J., Collins, J.C., Lungle, M.L., Mercer, G.D., 1969. Mechanism of ozonation reactions. IV. Carbon-nitrogen double bonds. J. Org. Chem. 34, 2961–2966.
Flyunt, R., Leitzke, A., Mark, G., Mvula, E., Reisz, E., Schick, R., von Sonntag, C., 2003. Determination of •OH, O2•-, and hydroperoxide yields in ozone reactions in aqueous solution. J. Phys. Chem. B 107, 7242–7253. https://doi.org/10.1021/jp022455b.
Frisch, M.J., Trucks, G.W., Schlegel, H.B., Scuseria, G.E., Robb, M.A., Cheeseman, J.R., Scalmani, G., Barone, V., Petersson, G.A., Nakatsuji, H., Li, X., Caricato, M., Marenich, A., Bloino, J., Janesko, B.G., Gomperts, R., Mennucci, B., Hratchian, H.P., Ortiz, J.V., Izmaylov, A.F., Sonnenberg, J.L., Williams-Young, D., Ding, F., Lipparini, F., Egidi, F., Goings, J., Peng, B., Petrone, A., Henderson, T., Ranasinghe, D., Zakrzewski, V.G., Gao, J., Rega, N., Zheng, G., Liang, W., Hada, M., Ehara, M., Toyota, K., Fukuda, R., Hasegawa, J., Ishida, M., Nakajima, T., Honda, Y., Kitao, O., Nakai, H., Vreven, T., Throssell, K., Montgomery Jr., J.A., Peralta, J.E., Ogliaro, F., Bearpark, M., Heyd, J.J., Brothers, E., Kudin, K.N., Staroverov, V.N., Keith, T., Kobayashi, R., Normand, J., Raghavachari, K., Rendell, A., Burant, J.C., Iyengar, S.S., Tomasi, J., Cossi, M., Millam, J.M., Klene, M., Adamo, C., Cammi, R., Ochterski, J.W., Martin, R.L., Morokuma, K., Farkas, O., Foresman, J.B., Fox, D.J., 2016. Gaussian 09, Revision D.01. Gaussian, Inc., Wallingford CT.
Goldstein, S., Samuni, A., 2007. Kinetics and mechanism of peroxyl radical reactions with nitroxides. J. Phys. Chem. A 111, 1066–1072. https://doi.org/10.1021/jp0655975.
Graeber, D., Boëchat, I.G., Encina-Montoya, F., Esse, C., Gelbrecht, J., Goyenola, G., Gücker, B., Heinz, M., Kronvang, B., Meerhoff, M., Nimptsch, J., Pusch, M.T., Silva, R.C.S., von Schiller, D., Zwirnmann, E., 2015. Global effects of agriculture on fluvial dissolved organic matter. Sci. Rep. 5. https://doi.org/10.1038/srep16328.
Hammes, F., Salhi, E., Köster, O., Kaiser, H.-P., Egli, T., von Gunten, U., 2006. Mechanistic and kinetic evaluation of organic disinfection by-product and assimilable organic carbon (AOC) formation during the ozonation of drinking water. Water Res. 40, 2275–2286. https://doi.org/10.1016/j.watres.2006.04.029.
Hariharan, P.C., Pople, J.A., 1973. The influence of polarization functions on molecular orbital hydrogenation energies. Theor. Chim. Acta 28, 213–222. https://doi.org/10.1007/BF00533485.
Hoigné, J., Bader, H., 1983. Rate constants of reactions of ozone with organic and inorganic compounds in water—II: dissociating organic compounds. Water Res. 17, 185–194.
Hoigné, J., Bader, H., 1978. Ozonation of water: kinetics of oxidation of ammonia by ozone and hydroxyl radicals. Environ. Sci. Technol. 12, 79–84.
Hoigné, J., Bader, H., Haag, W.R., Staehelin, J., 1985. Rate constants of reactions of ozone with organic and inorganic compounds in water—III. Inorganic compounds and radicals. Water Res. 19, 993–1004. https://doi.org/10.1016/0043-1354(85)90368-9.
Hübner, U., von Gunten, U., Jekel, M., 2015. Evaluation of the persistence of transformation products from ozonation of trace organic compounds – a critical review. Water Res. 68, 150–170. https://doi.org/10.1016/j.watres.2014.09.051.
Hwang, Y., Matsuo, T., Hanaki, K., Suzuki, N., 1995. Identification and quantification of sulfur and nitrogen containing odorous compounds in wastewater. Water Res. 29, 711–718. https://doi.org/10.1016/0043-1354(94)00145-W.
Ianni, J.C., 2017. Kintecus.
Ingold, K.U., Adamic, K., Bowman, D.F., Gillan, T., 1971. Kinetic applications of electron paramagnetic resonance spectroscopy. I. Self-reactions of diethyl nitroxide radicals. J. Am. Chem. Soc. 93, 902–908. https://doi.org/10.1021/ja00733a018.
Jámbor, A., Molnár-Perl, I., 2009. Amino acid analysis by high-performance liquid chromatography after derivatization with 9-fluorenylmethyloxycarbonyl chloride. J. Chromatogr. A 1216, 3064–3077. https://doi.org/10.1016/j.chroma.2009.01.068.
Johnson, D.H., Rogers, M.A.T., Trappe, G., 1956. 229. Aliphatic hydroxylamines. Part II. Autoxidation. J. Chem. Soc. 0, 1093–1103. https://doi.org/10.1039/JR9560001093.
Jonsson, M., Wayner, D.D.M., Lusztyk, J., 1996. Redox and acidity properties of alkyl- and arylamine radical cations and the corresponding aminyl radicals [1]. J. Phys. Chem. 100, 17539–17543. https://doi.org/10.1021/jp961286q.
Knoop, O., Hohrenk, L.L., Lutze, H.V., Schmidt, T.C., 2018. Ozonation of tamoxifen and toremifene – reaction kinetics and transformation products. Environ. Sci. Technol. 52, 12583–12591. https://doi.org/10.1021/acs.est.8b00996.
Krasner, S.W., Mitch, W.A., McCurry, D.L., Hanigan, D., Westerhoff, P., 2013. Formation, precursors, control, and occurrence of nitrosamines in drinking water: a review. Water Res. 47, 4433–4450. https://doi.org/10.1016/j.watres.2013.04.050.
Lange, F., Cornelissen, S., Kubac, D., Sein, M.M., von Sonntag, J., Hannich, C.B., Golloch, A., Heipieper, H.J., Möder, M., von Sonntag, C., 2006. Degradation of macrolide antibiotics by ozone: a mechanistic case study with clarithromycin. Chemosphere 65, 17–23. https://doi.org/10.1016/j.chemosphere.2006.03.014.
Le Lacheur, R.M., Glaze, W.H., 1996. Reactions of ozone and hydroxyl radicals with serine. Environ. Sci. Technol. 30, 1072–1080.
Lee, M., Blum, L.C., Schmid, E., Fenner, K., von Gunten, U., 2017. A computer-based prediction platform for the reaction of ozone with organic compounds in aqueous solution: kinetics and mechanisms. Environ. Sci.: Processes & Impacts 19, 465–476. https://doi.org/10.1039/C6EM00584E.
Lee, T.J., Taylor, P.R., 1989. A diagnostic for determining the quality of single-reference electron correlation methods. Int. J. Quantum Chem. 36, 199–207. https://doi.org/10.1002/qua.560360824.
Lee, Y., Escher, B.I., von Gunten, U., 2008. Efficient removal of estrogenic activity during oxidative treatment of waters containing steroid estrogens. Environ. Sci. Technol. 42, 6333–6339. https://doi.org/10.1021/es7023302.
Lee, Y., von Gunten, U., 2016. Advances in predicting organic contaminant abatement during ozonation of municipal wastewater effluent: reaction kinetics, transformation products, and changes of biological effects. Environ. Sci.: Water Res. Technol. 2, 421–442. https://doi.org/10.1039/C6EW00025H.
Leitzke, A., Reisz, E., Flyunt, R., von Sonntag, C., 2001. The reactions of ozone with cinnamic acids: formation and decay of 2-hydroperoxy-2-hydroxyacetic acid. J. Chem. Soc. Perkin Trans. 2, 793–797. https://doi.org/10.1039/b009327k.
Lester, Y., Mamane, H., Zucker, I., Avisar, D., 2013. Treating wastewater from a pharmaceutical formulation facility by biological process and ozone. Water Res. 47, 4349–4356. https://doi.org/10.1016/j.watres.2013.04.059.
Leverenz, H.L., Tchobanoglous, G., Asano, T., 2011. Direct potable reuse: a future imperative. J. Water Reuse Desal. 1, 2–10. https://doi.org/10.2166/wrd.2011.000.
Lipari, F., Swarin, S.J., 1982. Determination of formaldehyde and other aldehydes in automobile exhaust with an improved 2, 4-dinitrophenylhydrazine method. J. Chromatogr. A 247, 297–306.
Long, J.A., Harris, N.J., Lammertsma, K., 2001. Formaldehyde oxime ⇌ nitrosomethane tautomerism. J. Org. Chem. 66, 6762–6767. https://doi.org/10.1021/jo010671v.
Magdeburg, A., Stalter, D., Schlüsener, M., Ternes, T., Oehlmann, J., 2014. Evaluating the efficiency of advanced wastewater treatment: target analysis of organic contaminants and (geno-)toxicity assessment tell a different story. Water Res. 50, 35–47. https://doi.org/10.1016/j.watres.2013.11.041.
Marenich, A.V., Cramer, C.J., Truhlar, D.G., 2009. Universal solvation model based on

solute electron density and on a continuum model of the solvent defined by the bulk dielectric constant and atomic surface tensions. J. Phys. Chem. B 113, 6378–6396. https://doi.org/10.1021/jp810292n.
Markofsky, S.B., 2011. Nitro compounds, aliphatic. In: Wiley-VCH Verlag GmbH & Co KGaA (Ed.), Ullmann's Encyclopedia of Industrial Chemistry. Wiley-VCH Verlag GmbH & Co. KGaA, Weinheim, Germany. https://doi.org/10.1002/14356007.a17_401.pub2.
McCurry, D.L., Quay, A.N., Mitch, W.A., 2016. Ozone promotes chloropicrin formation by oxidizing amines to nitro compounds. Environ. Sci. Technol. 50, 1209–1217. https://doi.org/10.1021/acs.est.5b04282.
Mestankova, H., Escher, B., Schirmer, K., von Gunten, U., Canonica, S., 2011. Evolution of algal toxicity during (photo)oxidative degradation of diuron. Aquat. Toxicol. 101, 466–473. https://doi.org/10.1016/j.aquatox.2010.10.012.
Mitch, W.A., Sedlak, D.L., 2004. Characterization and fate of *N* -nitrosodimethylamine precursors in municipal wastewater treatment plants. Environ. Sci. Technol. 38, 1445–1454. https://doi.org/10.1021/es035025n.
Montgomery, J.A., Frisch, M.J., Ochterski, J.W., Petersson, G.A., 1999. A complete basis set model chemistry. VI. Use of density functional geometries and frequencies. J. Chem. Phys. 110, 2822–2827. https://doi.org/10.1063/1.477924.
Muñoz, F., Mvula, E., Braslavsky, S.E., von Sonntag, C., 2001. Singlet dioxygen formation in ozone reactions in aqueous solution. J. Chem. Soc. Perkin Trans. 2, 1109–1116. https://doi.org/10.1039/b101230o.
Muñoz, F., von Sonntag, C., 2000a. The reactions of ozone with tertiary amines including the complexing agents nitrilotriacetic acid (NTA) and ethylenediaminetetraacetic acid (EDTA) in aqueous solution. J. Chem. Soc. Perkin Trans. 2, 2029–2033. https://doi.org/10.1039/b004417m.
Muñoz, F., von Sonntag, C., 2000b. Determination of fast ozone reactions in aqueous solution by competition kinetics. J. Chem. Soc. Perkin Trans. 2, 661–664. https://doi.org/10.1039/a909668j.
Murray, R.W., Jeyaraman, R., Mohan, L., 1986. A new synthesis of nitro compounds using dimethyldioxirane. Tetrahedron Lett. 27, 2335–2336.
National Toxicology Program, 2016. Report on Carcinogens, fourteenth ed. U.S. Department of Health and Human Services, Public Health Service, Research Triangle Park, NC.
Naumov, S., von Sonntag, C., 2011. Standard Gibbs free energies of reactions of ozone with free radicals in aqueous solution: quantum-chemical calculations. Environ. Sci. Technol. 45, 9195–9204. https://doi.org/10.1021/es2018658.
Nöthe, T., Fahlenkamp, H., von Sonntag, C., 2009. Ozonation of wastewater: rate of ozone consumption and hydroxyl radical yield. Environ. Sci. Technol. 43, 5990–5995.
Olszyna, K., Heicklen, J., 1976. The inhibition of photochemical smog VI. The reaction of O3 with diethylhydroxylamine. Sci. Total Environ. 5, 223–230. https://doi.org/10.1016/0048-9697(76)90074-7.
Papajak, E., Zheng, J., Xu, X., Leverentz, H.R., Truhlar, D.G., 2011. Perspectives on basis sets beautiful: seasonal plantings of diffuse basis functions. J. Chem. Theory Comput. 7, 3027–3034. https://doi.org/10.1021/ct200106a.
Paradkar, V.M., Latham, T.B., Demko, D.M., 1995. Oxidative decarboxylation of α-amino acids with in situ generated dimethyl dioxirane. Synlett 1059–1060. https://doi.org/10.1055/s-1995-5174.
Pehlivanoglu-Mantas, E., Sedlak, D.L., 2006. Wastewater-derived dissolved organic nitrogen: analytical methods, characterization, and effects—a review. Crit. Rev. Environ. Sci. Technol. 36, 261–285. https://doi.org/10.1080/10643380500542780.
Pryor, W.A., Giamalva, D.H., Church, D.F., 1984. Kinetics of ozonation. 2. Amino acids and model compounds in water and comparisons to rates in nonpolar solvents. J. Am. Chem. Soc. 106, 7094–7100. https://doi.org/10.1021/ja00335a038.
Raghavachari, K., Trucks, G.W., Pople, J.A., Head-Gordon, M., 1989. A fifth-order perturbation comparison of electron correlation theories. Chem. Phys. Lett. 157, 479–483. https://doi.org/10.1016/S0009-2614(89)87395-6.
Ramseier, M.K., Peter, A., Traber, J., von Gunten, U., 2011. Formation of assimilable organic carbon during oxidation of natural waters with ozone, chlorine dioxide, chlorine, permanganate, and ferrate. Water Res. 45, 2002–2010. https://doi.org/10.1016/j.watres.2010.12.002.
Riebel, A.H., Erickson, R.E., Abshire, C.J., Bailey, P.S., 1960. Ozonation of carbon-nitrogen double bonds. I. Nucleophilic attack of ozone [1]. J. Am. Chem. Soc. 82, 1801–1807. https://doi.org/10.1021/ja01492a062.
Rios, A., Amyes, T.L., Richard, J.P., 2000. Formation and stability of organic zwitterions in aqueous solution: enolates of the amino acid Glycine and its derivatives. J. Am. Chem. Soc. 122, 9373–9385. https://doi.org/10.1021/ja001749c.
Roca-López, D., Tejero, T., Caramella, P., Merino, P., 2014. [2n2π + 2n2π] Cycloadditions: an alternative to forbidden [4π + 4π] processes. The case of nitrone dimerization. Org. Biomol. Chem. 12, 517–525. https://doi.org/10.1039/C3OB42014K.
Sacher, F., Lenz, S., Brauch, H.-J., 1997. Analysis of primary and secondary aliphatic amines in waste water and surface water by gas chromatography-mass spectrometry after derivatization with 2, 4-dinitrofluorobenzene or benzenesulfonyl chloride. J. Chromatogr. A 764, 85–93.
Sander, R., 2015. Compilation of Henry's law constants (version 4.0) for water as solvent. Atmos. Chem. Phys. 15, 4399–4981.
Sein, M.M., Zedda, M., Tuerk, J., Schmidt, T.C., Golloch, A., Sonntag, C. von, 2008. Oxidation of diclofenac with ozone in aqueous solution. Environ. Sci. Technol. 42, 6656–6662. https://doi.org/10.1021/es8008612.
Shah, A.D., Mitch, W.A., 2012. Halonitroalkanes, halonitriles, haloamides, and N-nitrosamines: a critical review of nitrogenous disinfection byproduct formation pathways. Environ. Sci. Technol. 46, 119–131. https://doi.org/10.1021/es203312s.
Smith, G.G., Sivakua, T., 1983. Mechanism of the racemization of amino acids. Kinetics of racemization of arylglycines. J. Org. Chem. 48, 627–634. https://doi.org/10.1021/jo00153a001.
Stalter, D., Magdeburg, A., Weil, M., Knacker, T., Oehlmann, J., 2010. Toxication or detoxication? In vivo toxicity assessment of ozonation as advanced wastewater treatment with the rainbow trout. Water Res. 44, 439–448. https://doi.org/10.1016/j.watres.2009.07.025.
Tekle-Röttering, A., Jewell, K.S., Reisz, E., Lutze, H.V., Ternes, T.A., Schmidt, W., Schmidt, T.C., 2016. Ozonation of piperidine, piperazine and morpholine: kinetics, stoichiometry, product formation and mechanistic considerations. Water Res. 88, 960–971. https://doi.org/10.1016/j.watres.2015.11.027.
Tentscher, P.R., Bourgin, M., von Gunten, U., 2018. Ozonation of *para* -substituted phenolic compounds yields *p* -Benzoquinones, other cyclic α,β-unsaturated ketones, and substituted catechols. Environ. Sci. Technol. 52, 4763–4773. https://doi.org/10.1021/acs.est.8b00011.
Ternes, T.A., Stüber, J., Herrmann, N., McDowell, D., Ried, A., Kampmann, M., Teiser, B., 2003. Ozonation: a tool for removal of pharmaceuticals, contrast media and musk fragrances from wastewater? Water Res. 37, 1976–1982. https://doi.org/10.1016/S0043-1354(02)00570-5.
Trogolo, D., Arey, J.S., Tentscher, P.R., 2019. Gas-phase ozone reactions with a structurally diverse set of molecules: barrier heights and reaction energies evaluated by coupled cluster and density functional theory calculations. J. Phys. Chem. A. https://doi.org/10.1021/acs.jpca.8b10323.
USEPA, 1985. Health and Environmental Effects Profile for Nitromethane (No. EPA/600/X-85/116 (NTIS PB88180518)). U.S. Environmental Protection Agency, Washington, D.C.
von Gunten, U., 2018. Oxidation processes in water treatment: are we on track? Environ. Sci. Technol. 52, 5062–5075. https://doi.org/10.1021/acs.est.8b00586.
von Gunten, U., 2003. Ozonation of drinking water: Part I. Oxidation kinetics and product formation. Water Res. 37, 1443–1467. https://doi.org/10.1016/S0043-1354(02)00457-8.
von Sonntag, C., von Gunten, U., 2012. Chemistry of Ozone in Water and Wastewater Treatment. IWA Publishing.
Wardman, P., 1989. Reduction potentials of one-electron couples involving free radicals in aqueous solution. J. Phys. Chem. Ref. Data 18, 1637–1755. https://doi.org/10.1063/1.555843.
Wayne, R.P., Pitts, J.N., 1969. Rate constant for the reaction O2(1Δg)+O3→2O2+O. J. Chem. Phys. 50, 3644–3645. https://doi.org/10.1063/1.1671606.
Westerhoff, P., Mash, H., 2002. Dissolved organic nitrogen in drinking water supplies: a review. J. Water Supply Res. Technol. - Aqua 51, 415–448. https://doi.org/10.2166/aqua.2002.0038.
WHO, 2005. Trihalomethanes in Drinking-Water. Background Document for Development of WHO Guidelines for Drinking-Water Quality (No. WHO/SDE/WSH/05.08/64). World Health Organization, Geneva.
Yang, L., Chen, Z., Shen, J., Xu, Z., Liang, H., Tian, J., Ben, Y., Zhai, X., Shi, W., Li, G., 2009. Reinvestigation of the nitrosamine-formation mechanism during ozonation. Environ. Sci. Technol. 43, 5481–5487. https://doi.org/10.1021/es900319f.
Zhao, Y., Truhlar, D.G., 2008. The M06 suite of density functionals for main group thermochemistry, thermochemical kinetics, noncovalent interactions, excited states, and transition elements: two new functionals and systematic testing of four M06-class functionals and 12 other functionals. Theoret. Chem. Acc. 120, 215–241. https://doi.org/10.1007/s00214-007-0310-x.
Zimmermann, S.G., Schmukat, A., Schulz, M., Benner, J., von Gunten, U., Ternes, T.A., 2012. Kinetic and mechanistic investigations of the oxidation of tramadol by ferrate and ozone. Environ. Sci. Technol. 46, 876–884. https://doi.org/10.1021/es203348q.
Zubarev, V., Brede, O., 1994. Direct detection of the cation radical of the spin trap a-phenyl-N-tert-butylnitrone. J. Chem. Soc. Perkin Trans. 2 0, 1821–1828.